Uterine progesterone signaling is a target for metformin therapy in polycystic ovary syndrome

Min Hu, MD PhD[1,†]; Yuehui Zhang, MD PhD[1,2,†]; Jiaxing Feng, MD[2,†]; Xue Xu, MD[2]; Jiao Zhang, MD[3]; Wei Zhao, MD[2]; Xiaozhu Guo, MD[2]; Juan Li, MD PhD[1,4]; Edvin Vestin, MD[1]; Peng Cui, MD[1,5,6]; Xin Li, MD PhD[1,7,8]; Xiao-ke Wu, MD PhD[2]; Mats Brännström, MD PhD[9]; Linus R. Shao, MD PhD[1]; Håkan Billig, MD PhD[1]

[1] Department of Physiology/Endocrinology, Institute of Neuroscience and Physiology, The Sahlgrenska Academy, University of Gothenburg, 40530 Gothenburg, Sweden; [2] Department of Obstetrics and Gynecology, Key Laboratory and Unit of Infertility in Chinese Medicine, First Affiliated Hospital, Heilongjiang University of Chinese Medicine, 150040 Harbin, China; [3] Department of Acupuncture and Moxibustion, Second Affiliated Hospital, Heilongjiang University of Chinese Medicine, 150040 Harbin, China; [4] Department of Traditional Chinese Medicine, The First Affiliated Hospital of Guangzhou Medical University, 510120 Guangzhou, China; [5] Department of Integrative Medicine and Neurobiology, State Key Lab of Medical Neurobiology, Shanghai Medical College and Institute of Acupuncture Research (WHO Collaborating Center for Traditional Medicine), Institute of Brain Science, Fudan University, 200032 Shanghai, China; [6] Institute of Integrative Medicine of Fudan University, 200032 Shanghai, China; [7] Department of Gynecology, Obstetrics and Gynecology Hospital of Fudan University, 200011 Shanghai, China; [8] Shanghai Key Laboratory of Female Reproductive Endocrine Related Diseases, 200011 Shanghai, China; [9] Department of Obstetrics and Gynecology, Sahlgrenska University Hospital, Sahlgrenska Academy, University of Gothenburg, 41345 Gothenburg, Sweden

† The authors consider that the first three authors should be regarded as joint first authors.

*** Present address, to where correspondence and reprint requests should be addressed**

Linus R. Shao, MD, PhD.
Department of Physiology/Endocrinology
Institute of Neuroscience and Physiology
The Sahlgrenska Academy at the University of Gothenburg
Medicinaregatan 11, P.O.Box 434
405 30 Göteborg
SWEDEN
Tel: +46 31-7863408

Fax: +46 31-7863512
E-mail: linus.r.shao@fysiologi.gu.se

CONFLICTS OF INTEREST: The authors indicate no potential conflicts of interest.

ACKNOWLEDGMENTS: This work was supported by the Swedish Medical Research Council (grant number 10380), the Swedish federal government under the LUA/ALF agreement (grant number ALFGBG-147791), the Jane and Dan Olsson's Foundation, the Hjalmar Svensson Foundation, and the Adlerbert Research Foundation to HB and RS as well as the National Natural Science Foundation of China (grant number 81303118), the Project of Young Innovation Talents in Heilongjiang Provincial University (grant number UNPYSCT-2015121), the project of Innovation Talents (Young Reserve Talents) in Harbin city (grant number 2015RAQYJ089), and the Project of Excellent Innovation Talents by Heilongjiang University of Chinese Medicine to YZ. The authors thank the Centre for Cellular Imaging at the University of Gothenburg and the National Microscopy Infrastructure (grant number VR-RFI 2016-00968) for providing assistance in microscopy.

RUNNING TITLE: Effects of metformin on progesterone signaling in the PCOS-like uterus

BACKGROUND: Impaired progesterone (P4) signaling is linked to endometrial dysfunction and infertility in women with polycystic ovary syndrome (PCOS). However, the molecular mechanisms behind this association are not well characterized. Metformin is one of the primary therapeutic drugs for PCOS patients, where beneficial treatment of endometrial dysfunction is observed clinically, but the effects of metformin on the regulation of the P4 signaling pathway are not fully understood.

OBJECTIVE: The present study sought to establish how the P4 signaling pathway is involved in improved uterine function in PCOS patients treated with metformin.

STUDY DESIGN: Patients were recruited and diagnosed with PCOS according to the Rotterdam criteria provided by the American Society for Reproductive Medicine and the European Society for Human Reproduction and Embryology. Endometrial biopsy samples were collected from non-PCOS patients with regular menstrual cycles and from PCOS patients with or without hyperplasia during the proliferative phase. Using an established PCOS-like rat model, which exhibits similar pathological alterations of both uterine morphology and function, we determined the molecular mechanism underlying metformin-induced alterations of P4 signaling molecules before and after implantation. To determine whether metformin directly regulates the expression and activity of progesterone receptor (PR), we evaluated PR isoform, PR-targeted, and implantation-related gene expression in an in vitro study of rat uterine tissues.

RESULTS: We found that in the absence of P4 or in the presence of sustained low levels of P4, both uterine PR isoforms were elevated in PCOS patients and in PCOS-like rats *in vivo*. This was positively associated with high levels of estrogen receptor (ER) expression. Consistent with mouse knockout studies, dysregulated expression of *Fkbp52 and Ncoa2*, two genes that contribute to uterine P4 resistance, was observed in PCOS-like rats before and after implantation. Our data showed that metformin directly suppressed uterine PR isoform

expression along with the correction of aberrant expression of PR-targeted and implantation-related genes in PCOS-like rats. Abnormal cell-specific regulation of PR and ER, paralleling the aberrant expression of PR-targeted and implantation-related genes, was retained in some PCOS-like rats with implantation failure. In addition, while increased PR expression was associated with inhibition of the MAPK/ERK/p38 signaling pathway, metformin treatment mainly restored the MAPK/p38 signaling pathway in PCOS-like rat uterus.

CONCLUSION: Our results suggest that the P4 signaling pathway might constitute the target of metformin treatment in PCOS patients with uterine dysfunction.

Key words: Metformin, progesterone receptor, MAPK/ERK/p38 signaling pathway, implantation, PCOS, infertility

Polycystic ovary syndrome (PCOS) is a clinically and etiologically heterogeneous hormone-imbalance disorder that is associated with multiple reproductive and metabolic abnormalities [1]. The incidence of PCOS varies between 5% and 20% of all reproductive-aged women depending on the ethnicity and diagnostic criteria applied [2]. Women suffering from PCOS present with arrested folliculogenesis and chronic anovulation-linked infertility [1, 2], and they also have more adverse reproductive risk as evidenced by an increase in the prevalence of implantation failure, recurrent miscarriage, spontaneous abortion, premature delivery, endometrial carcinoma [3-5]. In addition to the ovarian dysfunction [1, 2], it is assumed that the impairment of endometrial function also contributes to PCOS-associated infertility [6]. Although progesterone (P4)-based oral contraceptive therapy is often efficacious [7, 8], perturbations in endometrial P4 signaling that result from attenuated responsiveness and resistance to P4 are common in the endometrium of a PCOS patient [9, 10]. P4 resistance is a condition in which tissues and cells do not respond appropriately to P4 [11], and this is evidenced by endometriosis and endometrial hyperplasia that may progress to endometrial carcinoma despite supplementation with P4 or its analogs [12, 13]. Gene profiling experiments have shown that different endometrial genes are likely to act in concert in this abnormal condition in PCOS patients [14, 15]; however, how changes in the expression of P4 signaling molecules contribute to the P4 resistance in a PCOS patient's endometrium is poorly understood.

P4 is an essential contributing factor in female reproductive tissues that regulates multiple physiological processes such as the menstrual cycle, implantation, pregnancy maintenance, and labor initiation [6]. There are two major progesterone receptor (PGR) isoforms, PGRA and PGRB, both of which are involved in a common P4 signaling pathway for uterine cell-specific proliferation and differentiation [9, 16]. P4 binding activates both PGR isoforms and leads to translocation from the cytosol to the nucleus followed by binding to the P4-responsive

elements of the target genes, resulting in alterations of PGR-targeted gene expression depending on the recruitment of co-regulators [16]. It has been reported that the isoform-specific and endometrial cell-specific PGR expression fluctuates in humans during the menstrual cycle [9, 17]. Interestingly, defects in PGR isoform-specific P4 signaling in the uterus can give rise to distinct phenotypes of uterine impairment and implantation failure [9]. Although endometrial PGR expression is elevated in PCOS patients who have anovulation compared to PCOS patients who still ovulate and to non-PCOS patients [18, 19], whether endometrial PGR isoforms are individually up-regulated, along with the alteration of PGR-targeted gene expression, in PCOS patients is not known. Additionally, PGR activity is also modulated by the cytoplasmic mitogen-activated protein kinase (MAPK)/extracellular signal-regulated kinase (ERK) signaling pathway [16, 17]. While high levels of ERK1/2 expression and activation reflect the P4-PGR signaling-induced decidualization status in human and rodent uteri [20-22], it remains to be determined whether suppression of MAPK/ERK signaling occurs in the endometrium and whether such dysregulation can negatively impact uterine function under PCOS conditions.

Metformin is an anti-diabetic drug that is a clinically approved treatment in PCOS patients worldwide [23]. Several diverse molecular mechanisms of metformin have been demonstrated in human endometrial carcinoma tissues *in vivo* and in different endometrial cancer cells *in vitro* [4], and metformin's therapeutic effects on endometrial function are evidenced by improvement of endometrial receptivity, enhancement of endometrial vascularity and blood flow, and reversion of endometrial hyperplasia and carcinoma into normal endometria in some women with PCOS [24-26]. To date, several PCOS-like animal models have been developed to mimic the disease's clinical characteristics and to allow studies of pharmacological effects on specific tissues and biological processes [27]. Our recent studies using a PCOS-like rat model found that chronic treatment with metformin has significant anti-androgenic and anti-inflammatory impacts in the uterus [28]. Given the central role of P4 signaling in uterine

implantation [6, 16] and the ability of metformin to rescue implantation failure in some PCOS-like rats by modulating the expression of multiple implantation-related genes in the uterus *in vivo* [28], we speculated that the beneficial effects of metformin might be mechanistically linked to the uterine P4 signaling pathway under pathological conditions such as PCOS. To address this hypothesis, we analyzed PCOS-associated PGR isoform expression and the MAPK signaling network in human and rat uterine tissues. By combining a PCOS-like rat model [29] and *in vitro* tissue culture approach [30], we aimed to determine whether metformin directly reverses aberrant PGR-targeted and implantation-related gene expression in the PCOS-like rat uterus.

Materials and Methods

Study approval

All animal experiments were performed according to the National Institutes of Health guidelines on the care and use of animals and were approved and authorized by the Animal Care and Use Committee of the Heilongjiang University of Chinese Medicine, China (HUCM 2015-0112). Informed consent was obtained from all patients in accordance with a protocol reviewed and approved by the institutional ethical review board of the Obstetrics and Gynecology Hospital of Fudan University, Shanghai, China (OGHFU 2013-23).

Reagents and antibodies

Human recombinant insulin (Humulin NPH) was from Eli Lilly Pharmaceuticals (Giza, Egypt), and human chorionic gonadotropin (hCG) was from NV Organon (Oss, Holland). Metformin, anti-mouse IgG horseradish peroxidase (HRP)-conjugated goat (A2304), and anti-rabbit IgG HRP-conjugated goat (A0545) secondary antibodies were from Sigma-Aldrich (St. Louis, MO). Alexa Fluor 594-conjugated goat anti-mouse IgG (A21203), Alexa Fluor 488-

conjugated donkey anti-mouse IgG (A21202), and Alexa Fluor 488-conjugated goat anti-rabbit IgG (A11008) were from Invitrogen (Sollentuna, Sweden).

Patient selection and endometrial tissue collection

Reproductive-aged women (range, 25–45 years) with PCOS (n = 14) and without PCOS (n = 11) were originally recruited into the study. PCOS was diagnosed based on the Rotterdam criteria provided by the American Society for Reproductive Medicine and the European Society for Human Reproduction and Embryology [31]. All non-PCOS fertile women taking part in the investigation had regular menstrual cycles and showed no evidence of any pathological uterine disorder. Women with PCOS were excluded from this study if they had evidence of any chronic inflammatory disorders such as systemic lupus erythematosus, inflammatory bowel disease, rheumatoid arthritis, and asthma. Neither non-PCOS nor PCOS subjects were exposed to any hormonal or steroidal therapies within three months prior to tissues sampling [25, 32]. All endometrial tissues were obtained during the proliferative phase of the menstrual cycle by endometrial curettage of the bisected uteri obtained after hysterectomy for benign gynecological indications. Each endometrial sample was diagnosed and staged by routine pathology analysis based on standard histological criteria [33]. All samples were snap frozen in liquid nitrogen for subsequent RNA and protein analyses or fixed in 10% neutral formalin solution for 24 h at 4ºC and embedded in paraffin for histochemical analysis in a non-blinded manner.

Experimental animals and tissue preparations

Adult female Sprague–Dawley rats (n = 134) were obtained from the Laboratory Animal Centre of Harbin Medical University, Harbin, China (License number SCXK 2013-001). Animals were housed in the animal care facility with free access to food and water and a controlled temperature of 22°C ± 2°C with a 12 h light/dark cycle. Estrous cycles were monitored daily by vaginal lavage according to a standard protocol [34]. All rats (70 days old)

with the different stages of estrous cycle used in this study were confirmed by examination of vaginal smears under a light microscope for two sequential cycles (about 8–10 days). Any PCOS-like (insulin+hCG-treated) rats that exhibited prolonged estrous cycles (more than 5 days) were excluded from the study.

Experiment 1: Rats were randomly divided into control (saline treatment, n = 20) and experimental (PCOS-like, n = 20) groups. The experimental group was treated with insulin plus hCG to induce a PCOS-like metabolic and reproductive phenotype, and the control rats were treated with an equal volume of saline [29]. In brief, insulin was started at 0.5 IU/day and gradually increased to 6.0 IU/day between day 1 and the day 22 to induce hyperinsulinemia and insulin resistance, and 3.0 IU/day hCG was given on all 22 days to induce hyperandrogenism. Animals were treated with twice-daily subcutaneous injections until the end of the experiment. Rats with repeated insulin injections have not shown any hypoglycemic episodes [35-37]. Detailed analysis of endocrine and metabolic parameters as well as the uterine morphology in these animals has been reported previously [29]. On day 23, each group of rats was divided into two subgroups of 10 rats each (Supplemental Fig. 1A). For treatment, metformin was dissolved in saline and given as a daily oral dose of 500 mg/kg by a cannula. The treatment time and tissue collection are described in our previous study [28].

Experiment 2: Rats were randomly divided into control (saline treatment, n = 21) and experimental (PCOS-like, n = 15) groups and treated as described in Experiment 1 (Supplemental Fig. 1B). After metformin treatment, control and PCOS-like rats were mated with fertile vasectomized males of the same strain to induce implantation, which was determined by the presence of a vaginal plug (day 1 of pregnancy). The rats were sacrificed between 0800 and 0900 hours on day 6 of pregnancy. To identify the implantation sites, rats were injected intravenously with a Chicago Blue B dye solution (1% in saline) and sacrificed

10 min later. Uteri were dissected and assessed for clearly delineated blue bands as evidence of early implantation sites as described previously [28].

Experiment 3: Rats were divided into control (saline treatment, n = 9) and experimental (PCOS-like, n = 39) groups and treated as described in the Experiment 1. On the 23rd day, the PCOS-like rats were divided into four subgroups and treated daily with P4 (4 mg/kg), RU486 (6 mg/kg), or both for 3 days. For treatment, P4 and RU486 were dissolved in 100% ethanol and resuspended in sesame oil. All subcutaneous injections were in a volume of 100 µl. An equal volume of 100% ethanol and sesame oil was injected into both healthy control rats and PCOS-like rats as experimental controls (Supplemental Fig. 1C). The pharmacological doses and treatment time intervals of P4 and RU486 were chosen on the basis of previous studies [38, 39].

After dissection, the uterine horns were trimmed free of fat and connective tissue. One side of the uterus in each animal was fixed in 10% neutral formalin solution for 24 h at 4ºC and embedded in paraffin for histochemical analysis. The other side was immediately frozen in liquid nitrogen and stored at −70ºC for Western blot and quantitative real-time PCR (qRT-PCR) analysis.

Primary in vitro tissue culture and treatment

Uterine tissue culture and treatment was essentially carried out as described previously [30, 40]. After rinsing in cold PBS, uterine tissues obtained from control (n = 5) and PCOS-like (n = 5) rats were divided into equal-sized explants and placed in 24-well tissue culture plates (Sarstedt, Newton, MA) containing RPMI-1640 medium with charcoal-stripped 10% fetal calf serum and 100 IU/ml penicillin/streptomycin (GIBCO-BRL, San Francisco, CA). Cultured tissues treated with sterile saline or metformin (10 mM in sterile saline) were incubated in a humidified incubator (37ºC, 95% O_2, 5% CO_2) and separately collected at 0 h, 24 h, 48 h, and 72 h after treatment (Supplemental Fig. 2). Each culture condition was performed in five

replicates (five wells), and tissues from a minimum of five control rats and five PCOS-like (insulin+hCG-treated) rats were used. At the end of the experiments, cultured tissues were snap-frozen in liquid nitrogen and stored at –70°C.

Morphological assessment and immunostaining

Uterine tissues were fixed in 10% formalin, embedded in paraffin, and sectioned for hematoxylin and eosin staining according to standard procedures. Immunohistochemistry and immunofluorescence were performed according to previously described methods [28, 29]. The endogenous peroxidase and nonspecific binding were removed by incubation with 3% H_2O_2 for 10 min and with 10% normal goat serum for 1 h at room temperature. After incubation with the primary antibody (Supplemental Table 1) overnight at 4°C in a humidified chamber, the sections were stained using the avidin-biotinylated-peroxidase complex detection system (Vector Laboratories Inc., Burlingame, CA) followed by treatment with 3-amino-9-ethyl carbazole developing reagent plus High Sensitivity Substrate (SK-4200, Vector Laboratories). The sections were imaged on a Nikon E-1000 microscope (Japan) and photomicrographed using Easy Image 1 (Bergström Instrument AB, Sweden).

The other half of the uterine sections were incubated with primary antibody in 0.01 M Tris-buffered saline supplemented with Triton X-100 (TBST) containing 5% nonfat milk overnight at 4°C, and a secondary antibody was applied at room temperature for 1 h. After the sections were washed with TBST, they were re-suspended in mounting medium containing DAPI (4′,6′-diamidino-2-phenylindole; Vector Laboratories). Sections were examined under an Axiovert 200 confocal microscope (Zeiss, Jena, Germany) equipped with a laser-scanning confocal imaging LSM 710 META system (Carl Zeiss) and photomicrographed. Background settings were adjusted from the examination of negative control specimens. Images of positive staining were adjusted to make optimal use of the dynamic range of detection. The immune staining was quantified by semi-quantitative histogram scoring (Q-H score) as described

previously [41]. All morphological and immunohistochemical assays were performed by at least two researchers in an operator-blinded manner.

Protein isolation and Western blot analysis

A detailed explanation of the Western blot analysis protocol has been published [28, 29]. Total protein was isolated from whole uterine tissue by homogenization in RIPA buffer (Sigma-Aldrich) supplemented with cOmplete Mini protease inhibitor cocktail tablets (Roche Diagnostics, Mannheim, Germany) and PhosSTOP phosphatase inhibitor cocktail tablets (Roche Diagnostics). After determining total protein by Bradford protein assay, equal amounts (30 μg) of protein were resolved on 4–20% TGX stain-free gels (Bio-Rad Laboratories GmbH, Munich, Germany) and transferred onto PVDF membranes. The membranes were probed with the primary antibody (Supplemental Table 1) in TBST containing 5% non-fat dry milk followed by HRP-conjugated secondary antibody. When necessary, the PVDF membranes were stripped using Restore PLUS Western blot stripping buffer (Thermo Scientific, Rockford, IL) for 15 minutes at room temperature, washed twice in TBST, and then re-probed. Ultraviolet activation of the Criterion stain-free gel on a ChemiDoc MP Imaging System (Bio-Rad) was used to control for proper loading. Band densitometry was performed using Image Laboratory (Version 5.0, Bio-Rad).

RNA extraction and qRT-PCR analysis

For RNA isolation, tissues from each rat were lysed using TRIzol Reagent (Life Technologies), and RNA was isolated following standard protocols. qRT-PCR was performed with a Roche Light Cycler 480 sequence detection system (Roche Diagnostics Ltd., Rotkreuz, Switzerland) as previously described [28, 29]. The PCR amplifications were performed with a SYBR green qPCR master mix (#K0252, Thermo Scientific, Rockford, IL). Total RNA was prepared from the frozen whole uterine tissues, and single-stranded cDNA was synthesized from each sample (2 μg) with M-MLV reverse transcriptase (#0000113467, Promega

Corporation, Fitchburg, WI) and RNase inhibitor (40 U) (#00314959, Thermo Scientific). cDNA (1 µl) was added to a reaction master mix (10 µl) containing 2× SYBR green qPCR reaction mix (Thermo Scientific) and gene-specific primers (5 µM each of forward and reverse primers). All primers are indicated in Supplemental Table 2. All reactions were performed six times, and each reaction included a non-template control. The results for target genes were expressed as the amount relative to the average CT values of *ACTB* + *CYC1* (humans) or *GAPDH* + *U87* (rats) in each sample. Relative gene expression was determined with the 2−ΔΔCT method, and the efficiency of each reaction – as determined by linear regression – was incorporated into the equation. The qRT-PCR results obtained from human endometria were validated by either Western blot analysis or immunohistochemical and immunofluorescence assays.

Measurement of biochemical parameters

Concentrations of gonadotropins (follicle stimulating hormone and luteinizing hormone), steroid hormones (17β-estradiol, progesterone, testosterone, 5α-dihydrotestosterone, and androstenedione), sex hormone-binding globulin, glucose, and insulin in rat serum samples were measured using commercially available assays (Cloud-Clone Corp., Houston, TX) as described previously [28]. All samples and standards were measured in duplicate. The intra- and inter-assay coefficients of variation are listed in Supplemental Table 3.

Statistical analysis

GraphPad Prism was used for statistical analysis and graphing. For all experiments, n-values represent the number of individual animals. Data are represented as the means ± SEM. Statistical analyses were performed using SPSS version 24.0 statistical software for Windows (SPSS Inc., Chicago, IL). The normal distribution of the data was tested with the Shapiro–Wilk test. Differences between groups were analyzed by one-way ANOVA or two-way ANOVA, and this was followed by Tukey's post-hoc test for normally distributed data or the

Kruskal–Wallis test followed by the Mann–Whitney U-test for skewed data. All *p*-values less than 0.05 were considered statistically significant.

Results

Elevation of endometrial PGR isoform expression in PCOS patients

Our qRT-PCR data indicated that endometrial mRNA levels of both PGR isoforms were higher in PCOS patients than non-PCOS patients in the proliferative phase of the menstrual cycle (Fig. 1A), and Western blot analysis showed that the protein levels of PGRA were also elevated in PCOS patients compared to non-PCOS patients (Fig. 1B). Additionally, immunohistochemical analysis revealed that although the positive nuclear staining for PGR and PGRB in the epithelia and stroma was detected in non-PCOS patients, significantly increased immunoreactivity of PGR and PGRB in the epithelia and stroma was found in PCOS patients (Fig. 1C). These results suggested that alterations of endometrial PGR expression in PCOS patients might be accounted for by the overall induction of total PGR protein, particularly by increased PGRA protein expression. We and others have shown that the expression of uterine estrogen receptor (ER) α, cytokeratin 8, vimentin, and Ki-67 proteins are altered in PCOS patients and in PCOS-like rats [10, 29, 42]. To further characterize the endometrial phenotypes in our samples, the expression profiles of several potential molecular markers (ERα, cytokeratin 8, vimentin, and Ki-67) was evaluated. As shown in Figure 1B and 1C, although endometrial ERα protein level varied among individuals with no significant changes between non-PCOS and PCOS patients by Western blot analysis, a general increase in ERα protein expression was identified in PCOS patients compared to non-PCOS patients using the immunofluorescence assay. There were no obvious changes in cytokeratin 8 protein levels in non-PCOS and PCOS patients. Concurrently, we observed that increased vimentin

expression was associated with increased immunoreactivity of Ki-67 in the glandular epithelia in PCOS patients (Fig. 1B and C).

Metformin alters PGR isoform and PGR-targeted gene expression in PCOS-like rats

The insulin+hCG-treated rats exhibit reproductive disturbances that mimic human PCOS [28, 29]. Prompted by these findings, we set out to investigate the impact of P4 signaling in this model. First, we showed that although the ratio of PGRA to PGRB was not significantly different between control and PCOS-like rats, the PCOS-like rats had increased levels of uterine PGRA and PGRB (Fig. 2A). While PGR immunoreactivity was primarily evidenced in control rat uterine luminal and glandular epithelia as well as in the stroma, the immunoreactivity of luminal epithelial PGR expression was associated with increased numbers of luminal epithelial cells and increased immunoreactivity of PGR in the stroma in PCOS-like rats (Fig. 2B). Metformin treatment did not significantly affect PGR isoform expression in control rats and PCOS-like rats compared to those rats treated with saline (Fig. 2A). However, we found that PGR immunoreactivity was decreased in the luminal and glandular epithelia by metformin treatment in both control rats and PCOS-like rats compared to those treated with saline (Fig. 2B). Conversely, intense immunoreactivity of PGR expression was detected in the stroma located close to the luminal epithelia in control and PCOS-like rats treated with metformin (Fig. 2B). In contrast to the epithelia and stroma, no significant changes in PGR expression in the myometrium were found in any of the groups (data not shown). Because a large body of evidence indicates that regulation of P4 signaling results in changes in the expression of several PGR-targeted genes in the uterus [43], we profiled the expression of genes that are indicators for PGR activity in the rat uterus by qRT-PCR. Quantitative data indicated that *Ihh*, *Smo*, and *Nr2f2* mRNA levels were increased in PCOS-like rats compared to control rats treated with saline. In contrast, the *Fkbp52* mRNA level was decreased in PCOS-like rats compared to control rats (Fig. 2C). We next determined the actions of metformin treatment on

PGR-targeted gene expression and showed that *Ptch*, *Fkbp52*, and *Ncoa2* levels were increased in PCOS-like rats treated with metformin compared to PCOS-like rats treated with saline, while *Smo* and *Nr2f2* mRNA levels were decreased on PCOS-like rats treated with metformin compared to those treated with saline (Fig. 4).

Metformin partially prevents implantation failure in parallel with regulation of PGR isoform and PGR-targeted gene expression in PCOS-like rats

Metformin has been shown to partially rescue the disruption of the implantation process in PCOS-like rats [28], and the altered endocrine and metabolic parameters in these animals are shown in Supplemental Table 4. After metformin treatment, total testosterone levels, the ratio of total testosterone to androstenedione, and fasting insulin levels were all significantly higher in PCOS-like rats where implantation did not occur compared to those with implantation, as was insulin resistance as assessed by the homeostasis model assessment of insulin resistance, mirroring the endocrine and metabolic abnormalities in PCOS patients [1, 2]. Of note, PCOS-like rats that failed to implant embryos also exhibited decreased P4 levels. These data suggest that implantation failure in PCOS-like rats treated with metformin is due not only to hyperandrogenism and insulin resistance, but also to impairment of P4 signaling in the uterus. Further morphological characterization of metformin-treated PCOS-like rats with no implantation revealed the infiltration of immune cells into the glandular epithelial cell layer in a similar manner to when hormone imbalances were studied in a previous report [44] (Supplemental Fig. 3, black arrowheads). To determine how impairment of P4 signaling causes implantation failure, we subsequently analyzed PGR isoform and PGR-targeted gene expression in PCOS-like rats with no implantation. Although treatment with metformin increased PGR isoform expression in control and PCOS-like rats, neither the PGRA nor PGRB protein level was altered between PCOS-like rats with implantation and with failed implantation (Fig. 3A). As shown in Figure 3B, while PGR protein was expressed in the

decidualizing stroma at the site of implantation in all groups, PGR immunoreactivity was increased in the stroma of the inter-implantation region in control rats treated with metformin. Furthermore, we found that the immunoreactivity of PGR was increased in the epithelia in PCOS-like rats without implantation despite metformin treatment. Thus, metformin appeared to participate in the regulation of uterine PGR expression in a cell type-specific manner in PCOS-like rats before and after implantation. qRT-PCR data indicated that *Ihh* and *Ncoa2* mRNAs were increased and that *Ptch* and *Fkbp52* mRNAs were decreased in metformin-treated PCOS-like rats with no implantation compared to control rats treated with saline or metformin and to metformin-treated PCOS-like rats with implantation (Fig. 3C).

Metformin directly regulates PGR isoform, PGR-target, and implantation-related gene expression in vitro

Based on these *in vivo* observations, we asked whether the effect of metformin was direct or indirect in the PCOS-like rat uterus. *In vitro* uterine tissue culture experiments revealed that *Pgr* and *Pgrb*, mRNA levels were higher in PCOS-like rats compared to control rats, in agreement with alteration of PGR isoform protein expression (Fig. 2C). Furthermore, metformin treatment increased *Pgr* and *Pgrb* mRNA levels in control and PCOS-like rats in a time-dependent manner (Fig. 4). Consistent with the *in vivo* effects of metformin in PCOS-like rats (Fig. 2C), *Ihh*, *Smo*, and *Nr2f2* mRNA levels were increased in the PCOS-like rat uterus compared to the control rat uterus and were down-regulated by metformin treatment *in vitro*. While the *Hand2* mRNA level was upregulated by metformin treatment at 48 h and 72 h, we detected the upregulation of *Ptch*, *Fkbp52*, and *Ncoa2* mRNA levels in the PCOS-like rat uterine tissues over a 72-h course after metformin treatment (Fig. 4).

The expression of a number of implantation-related genes has been reported to be regulated by metformin treatment in PCOS-like rats during implantation [28]. These previous observations prompted further analysis of implantation-related gene expression by metformin

treatment *in vitro*. In contrast to the different regulation patterns of *Spp1*, *Lrh1*, *Sgk1*, and *Krt13* mRNAs under *in vivo* and *in vitro* conditions, the *in vitro* responses of uterine *Prl*, *Igfbp1*, *Il11*, *Pc6*, *Maoa*, *Ednrb*, *Hoxa10*, *Hoxa11*, and *Hbegf* mRNA levels to metformin (Fig. 5) were coincident with the *in vivo* regulation of the expression pattern of these genes [28]. Our data indicated that metformin directly up-regulates uterine *Prl*, *Maoa*, *Ednrb*, and *Hbegf* mRNA levels in PCOS-like rats during implantation *in vivo*.

To ascertain whether the modulation of uterine gene expression is P4-mediated and PGR-dependent in PCOS-like rats, insulin+hCG-treated rats were injected subcutaneously with P4 and/or RU 486 for three days. As shown in Figure 6, the increased PGR isoform protein levels (Fig. 2A) were confirmed by analysis of *Pgr* and *Pgrb* mRNA expression in the PCOS-like rat uterus. Although treatment with P4 and/or RU486 did not significantly affect *Pgr* mRNA expression, we found that *Pgrb* mRNA levels were decreased in PCOS-like rats compared to those rats with no treatment (Fig. 6). Among seven PGR-targeted genes (Fig. 2C), we found that *Ptch*, *Hand2*, and *Fkbp52* mRNA levels were increased and that *Ihh*, *Smo*, and *Nr2f2* mRNA levels were decreased in PCOS-like rats treated with P4 compared to those rats with no treatment. We also observed that treatment with RU486 alone or combined with P4 reversed the changes in *Smo*, *Hand2*, and *Fkbp52* mRNA levels in PCOS-like rats (Fig. 6). No significant differences of uterine *Ncoa2* mRNA expression were observed in PCOS-like rats regarding the different treatments. Based on our current experimental approaches, it is likely that another regulatory mechanism contributes to the metformin-induced up-regulation of *Ncoa2* mRNA levels in PCOS-like rats.

Metformin regulates the MAPK signaling pathway in PCOS-like rats before and after implantation

In an attempt to understand the changes in PGR activation and function observed in PCOS patients [16], we performed a Western blot analysis to measure the expression of several

proteins that are involved in the MAPK signaling pathway in the uterus after metformin treatment. As shown in Figure 7A, there was no significant difference in p-c-Raf, p-MEK1/2, p-ERK1/2, p-p38 MAPK, or p38 MAPK expression between saline-treated and metformin-treated rats. Quantitative protein data indicated that the expression of p-p38 MAPK and p38 MAPK was significantly decreased in PCOS-like rats compared to control rats. Nevertheless, metformin treatment only reversed p-p38 MAPK protein expression in PCOS-like rats.

We next assessed whether the MAPK/ERK signaling pathway contributes to uterine implantation in control and PCOS-like rats treated with metformin. As shown in Figure 7B, although the p-MEK1/2 level was decreased in control rats treated with metformin compared to control rats treated with saline, no significant difference in p-c-Raf, p-ERK1/2, ERK1/2, p-p38 MAPK, or p38 MAPK expression between these two groups was found. Furthermore, our data showed that p-c-Raf, p-MEK1/2, and p-ERK1/2 protein levels were down-regulated in PCOS-like rats treated with metformin regardless of the occurrence of implantation. We also found that after metformin treatment PCOS-like rats with implantation exhibited decreased p-p38 MAPK, but not p38 MAPK, expression. We failed to find any activation of Jun N-terminal kinase (JNK), a member of the MAPK family, in control or PCOS-like rats treated with metformin regardless of implantation (data not shown).

Up-regulation of estrogen receptor (ER) expression in PCOS-like rats can be suppressed by metformin

Because estrogen-ER signaling regulates uterine PGR expression and activity [9, 16] and because increased circulating E2 in PCOS-like rats can be inhibited by metformin treatment [28], we sought to determine whether ER subtypes (ERα and ERβ) are involved in the regulation of aberrant PGR expression in PCOS-like rats and, if so, if metformin possibly alters ER subtype expression. Our data showed that PCOS-like rats exhibited increased *Esr1* (ERα) and *Esr2* (ERβ) mRNA levels, which were suppressed by metformin treatment. As shown in Figure 8A,

while nuclear ERα immunoreactivity was detected in the epithelia and stroma in control rats treated with saline (Fig. 8B1), immunoreactivity of ERα was increased in the glandular epithelia and stroma in PCOS-like rats (Fig. 8D1). Furthermore, treatment with metformin led to decreased ERα immunoreactivity in control (Fig. 8C1) and PCOS-like rats (Fig. 8E1). No obvious difference in ERα immunoreactivity was observed in the myometrium in any of the groups (Fig. 8B2-E2). We also found that ERβ was mainly co-localized with ERα in the epithelia and stroma but not in the myometrium in control and PCOS-like rats regardless of the different treatments. Furthermore, with metformin treatment, we noted a significant increase in uterine *Esr1* and *Esr2* mRNAs in PCOS-like rats without implantation (Fig. 9A). Immunofluorescence staining revealed that, overall, immunoreactivities of both ERα and ERβ were diminished in the decidualizing stroma at the site of implantation (Fig. 9B1–D1), in the epithelia and stroma of the inter-implantation region (Fig. 9B2–D2) in control rats treated with saline or metformin (Fig. 9B2–C2), and in the inter-implantation site of PCOS-like rats treated with metformin (Fig. 9D2) compared to those rats before implantation (Fig 8. B1–E2). Interestingly, PCOS-like rats with no implantation exhibited sustained nuclear ERα immunoreactivity in the glandular epithelia and stroma (Fig. 9E1).

Differential cell-specific expression of phospho-histone H3 in PCOS-like rats treated with metformin

As previously demonstrated [42], p-histone H3 is of special interest because the endometrium of PCOS patients displays high levels of p-histone H3, which is associated with cellular processes such as mitosis [45]. Quantitative assessment of p-histone H3 indicated that no significant change in p-histone H3 immunoreactivity was present in the epithelia or stroma in any of groups (Supplemental Fig. 4E); however, metformin treatment decreased p-histone H3 immunoreactivity in the myometrium in PCOS-like rats compared to those treated with saline. Of note, intensely p-histone H3-positive stromal cells close to the luminal and glandular

epithelia were found in PCOS-like rats treated with metformin (Supplemental Fig. 4D2). Similarly, p-histone H3 immunoreactivity was significantly increased in the stroma at the inter-implantation sites in PCOS-like rats treated with metformin independently of implantation (Supplemental Fig. 5E). In PCOS-like rats without implantation, p-histone H3 immunoreactivity was often detected in the luminal epithelia (Supplemental Fig. 5D1), although this was not statistically significant compared to PCOS-like rats with implantation (Supplemental Fig. 5E). It is thus likely that the regulation of mitotic activity by metformin is cell type-dependent in the uterus.

Comment

Reproductive dysfunction and infertility manifest noticeably in PCOS patients [6]. In striking contrast to the attention given to hyperandrogenism and insulin resistance in women with PCOS, the aberrant P4 signaling pathway resulting in uterine P4 resistance has received much less attention [9, 10]. This study is the first to show that the therapeutic effects of metformin on the regulation of uterine function in PCOS-like rats is mediated through P4 signaling.

Elucidating the regulation of endometrial PGR levels under PCOS conditions is important clinically. Our data show that increased PGR expression is associated with elevated ER expression in the endometrium of PCOS patient. A similar expression pattern of PGR and ER in PCOS-like rats, in association with an increased circulating E2 level [29], suggests that E2-ER signaling contributes to the up-regulation of PGR under PCOS conditions *in vivo*. Similar to PCOS patients, PCOS-like rats also displayed high levels of PGR isoforms and ER subtypes in the uterus. The induction of implantation is required for the activation of PGR, and implantation subsequently alters gene expression in the endometrium [16, 17]; however, PGR-targeted gene expression in PCOS patients and PCOS-like rats has only been demonstrated to a limited degree. The current study shows that significantly decreased

Fkbp52 gene expression parallels increased expression of *Ihh*, *Smo*, and *Nr2f2* mRNAs without changes in *Ncoa2* mRNA in PCOS-like rats. In addition, we also found that abnormal expression of PGR-target genes, including *Fkbp52* and *Ncoa2*, is retained in PCOS-like rats with implantation failure. This is supported by *in vivo* studies showing that mice lacking *Fkbp52* [46, 47] or *Ncoa2* [48, 49] demonstrate the absence of decidualization after P4 supplementation due to diminished P4 responsiveness. Previous studies have reported that women with endometriosis and endometrial hyperplasia/carcinoma who develop P4 resistance have low levels of PGR expression [12, 13]. Although it is currently unclear why differences exist in the regulation of uterine PGR expression between different diseases with P4 resistance, it is likely that uterine P4 resistance in PCOS-like rats is due to impaired PGR activity rather than PGR expression. We must emphasize that the array of P4-regulated and implantation-related genes were measured in the total uterine content in our current experiments. Therefore, some cell type-specific genes that would be transiently altered might have been missed.

Previous work from our laboratory and others has shown that metformin therapy has a significant impact on endometrial function in PCOS patients [24-26] and in PCOS-like rats [28]. The strength of our study is to depict the actions of metformin in the PCOS-like rat uterus before and after implantation. We demonstrate that metformin has a direct effect on the regulation of PGR expression and on PGR-targeted and implantation-related gene expression under PCOS conditions. Functionally, our data show that metformin not only suppresses epithelial cell-specific PGR expression in contrast to ERα expression, but that it also corrects the abnormal levels of PGR-targeted genes (*Ihh*, *Ptch*, *Fkbp52*, and *Ncoa2*) in PCOS-like rats with implantation. These results also lend support for the idea that dysregulated P4 resistance-related gene expression contributes to the uterine dysfunction in PCOS-like rats, although more studies are needed to dissect the mechanistic reasons for individual gene-induced P4 resistance under PCOS conditions *in vivo*. On the other hand, the implantation in mammals

requires other factors in addition to PGR and PGR-target genes, and aberrations in these factors can also cause reproductive failure (46, 47). Our previous study has demonstrated that if metformin treatment fails to correct several implantation-related genes (*Prl*, *Maoa*, *Ednrb*, and *Hbegf*) in PCOS-like rats, those animals will still exhibit implantation failure [28]. Having shown in the present study that metformin treatment directly regulates these genes as initially seen in PCOS-like rats *in vitro*, it is expected that metformin can regulate multiple signaling molecules in addition to those involved in P4 signaling and that this in turn will affect overall uterine function leading to implantation in PCOS-like rats. Our studies demonstrate how metformin influences the uterine implantation process in addition to suppression of hyperandrogenism and insulin resistance [28]. However, the molecular details from this study are mainly derived from PCOS-like rats, and thus it will be of interest to determine whether long-term treatment with metformin in PCOS patients with endometrial defects also overcomes P4 resistance and subfertility or infertility by correcting PGR-targeted and implantation-related gene expression in these patients.

Importantly, chronic inflammation has been shown to be closely correlated to high inflammatory mediator production under PCOS conditions [2]. For example, there is a noticeable increase in the inflammatory cytokines such as IL-6 and TNFα in the peripheral circulation of PCOS patients [50, 51]. Similarly, several studies by our laboratory and others have described increased gene expression of *IL-6*, *TNFα*, and *Mcp-1* (*CCL-2*) in PCOS patient endometrium and the PCOS-like rat uterus [10, 28, 52-54]. Moreover, P4 has been shown to suppress TNFα-stimulated IL-6 and Mcp-1 production in human endometriotic stromal cells *in vitro* [55]. These findings suggest that the PCOS-induced uterine inflammation might be inhibited by activation of P4 signaling. However, although several hypothesized mechanisms that might explain how hyperandrogenism and insulin resistance themselves contribute to systemic inflammatory responses [56, 57], interference between the metabolic dysfunction-

induced and intrauterine PGR-dependent inflammation under PCOS conditions has not yet been demonstrated. Notably, our experiments combined with qRT-PCR and Western blot analyses provide compelling evidence that the aberrant regulation of uterine PGR isoforms is not only possible, but would likely be PGR-dependent in PCOS-like rats. Therefore, while both PGR isoforms appear to be involved in the uterine inflammatory signaling pathways [16], our results raise the interesting possibility that significant cross talk between PGRA and PGRB might coordinate uterine inflammatory responses in PCOS patients who are lacking P4 and/or suffering from P4 resistance. Because both isoforms function as transcriptional factors leading to the distinct and overlapping signaling pathways needed to maintain uterine function [9, 16], further studies using PGR isoform-specific knockout female mice treated with insulin and hCG (PCOS-like) will be required to clarify the precise role of individual PGR isoform in the inflammation stages of uterine P4 resistance under PCOS conditions.

P4-mediated and PGR-dependent regulation of ERK1/2 expression plays a critical role in humans and rodents during endometrial decidualization and implantation [20-22], but such regulation under PCOS conditions has not previously been reported. The inhibition of ERK1/2 expression and activation has been reported in ovarian granulosa and thecal cells in PCOS patients [58, 59], and we have previously shown that the expression and activation of uterine ERK1/2 is suppressed in rats treated with insulin and hCG to induce the PCOS phenotype [29]. The present study supports and extends this work. Here we observed no changes in p-ERK1/2 or ERK1/2 expression in the rat uterus after prolonged treatment with insulin and hCG. However, we observed that the levels of p-c-Raf and p-MEK1/2, two upstream regulators of ERK1/2, were significantly decreased in PCOS-like rats after uterine implantation, establishing a tight link between different MAPK/ERK signaling molecules. Our data suggest that regulation of uterine ERK1/2 expression *in vivo* is time-dependent [20-22], which is similar to the regulation of PGR isoforms and PGR-targeted gene expression. The

MAPK/ERK/p38 signaling pathway contributes to the regulation of inflammation and cytokine production [60, 61], and the dysregulation of inflammation-related molecules is associated with PCOS conditions [52-54, 62]. Furthermore, like the activation of NFκB signaling that induces the transcriptional levels of inflammation-related gene expression in ovarian granulosa cells and in serum in PCOS patients [51, 63], our previous study has shown that the sustained metformin treatment markedly suppresses uterine inflammatory gene expression, especially the *Il-6* and *TNFα* mRNAs that are associated with inhibition of nuclear NFκB translocation in PCOS-like rats [28]. Importantly, p38 can antagonize ERK1/2 signaling mediated by protein phosphatase 2A and consequently down-regulate inflammatory cytokine and chemokine production [61], and the anti-inflammatory effects of MAPK/p38 are involved in the regulation of NFκB activity [60]. These observations further indicate that metformin inhibits NFκB-driven inflammatory processes through p38 activation rather than through ERK1/2 inhibition in the PCOS-like rat uterus. However, the question of whether such metformin-induced regulation of MAPK/ERK/p38 signaling depends on uterine PR expression and activity under PCOS conditions remains to be determined.

The results of the present study permit us to draw the following conclusions. 1) In the absence of P4 or with sustained low levels of P4, the expressions of both uterine PGR isoforms are elevated in PCOS patients and PCOS-like rats *in vivo*. This is positively associated with the high levels of ERs in PCOS patients and PCOS-like rats. Consistent with mouse knockout studies, altered expression of *Fkbp52* and *Ncoa2*, two genes that contribute to uterine P4 resistance, is seen in PCOS-like rats before and after implantation. 2) Metformin directly suppresses uterine PGR isoform expression along with the correction of aberrant expression of PGR-targeted and implantation-related genes in PCOS-like rats. Abnormal cell-specific regulation of PGR and ER, paralleling the aberrant expression of PGR-targeted and implantation-related genes, is retained in PCOS-like rats with implantation failure. 3)

Increased PGR expression is associated with inhibition of the MAPK/ERK/p38 signaling pathway, and the primary effect of metformin treatment is to restore the MAPK/p38 signaling pathway in the PCOS-like rat uterus. Taken together, our findings provide support for metformin therapy in the improvement of P4 signaling in PCOS-like rats with uterine dysfunction and for its clinical relevance in the treatment of PCOS patients with P4 resistance.

REFERENCES

1. ROSENFIELD RL, EHRMANN DA. The Pathogenesis of Polycystic Ovary Syndrome (PCOS): The Hypothesis of PCOS as Functional Ovarian Hyperandrogenism Revisited. Endocr Rev 2016;37:467-520.
2. AZZIZ R, CARMINA E, CHEN Z, et al. Polycystic ovary syndrome. Nat Rev Dis Primers 2016;2:16057.
3. PALOMBA S, DE WILDE MA, FALBO A, et al. Pregnancy complications in women with polycystic ovary syndrome. Hum Reprod Update 2015;21:575-92.
4. SHAO R, LI X, FENG Y, et al. Direct effects of metformin in the endometrium: a hypothetical mechanism for the treatment of women with PCOS and endometrial carcinoma. J Exp Clin Cancer Res 2014;33:41.
5. GOODARZI MO, DUMESIC DA, CHAZENBALK G, AZZIZ R. Polycystic ovary syndrome: etiology, pathogenesis and diagnosis. Nat Rev Endocrinol 2011;7:219-31.
6. EVANS J, SALAMONSEN LA, WINSHIP A, et al. Fertile ground: human endometrial programming and lessons in health and disease. Nat Rev Endocrinol 2016;12:654-67.
7. VRBIKOVA J, CIBULA D. Combined oral contraceptives in the treatment of polycystic ovary syndrome. Hum Reprod Update 2005;11:277-91.
8. LOPES IM, MAGANHIN CC, OLIVEIRA-FILHO RM, et al. Histomorphometric Analysis and Markers of Endometrial Receptivity Embryonic Implantation in Women With Polycystic Ovary Syndrome During the Treatment With Progesterone. Reprod Sci 2014;21:930-38.
9. LI X, FENG Y, LIN JF, BILLIG H, SHAO R. Endometrial progesterone resistance and PCOS. J Biomed Sci 2014;21:2.
10. PILTONEN TT. Polycystic ovary syndrome: Endometrial markers. Best Pract Res Clin Obstet Gynaecol 2016;37:66-79.
11. CHROUSOS GP, MACLUSKY NJ, BRANDON DD, et al. Progesterone resistance. Adv Exp Med Biol 1986;196:317-28.
12. SHAO R, CAO S, WANG X, FENG Y, BILLIG H. The elusive and controversial roles of estrogen and progesterone receptors in human endometriosis. Am J Transl Res 2014;6:104-13.
13. GUNDERSON CC, FADER AN, CARSON KA, BRISTOW RE. Oncologic and reproductive outcomes with progestin therapy in women with endometrial hyperplasia and grade 1 adenocarcinoma: a systematic review. Gynecol Oncol 2012;125:477-82.
14. SAVARIS RF, GROLL JM, YOUNG SL, et al. Progesterone resistance in PCOS endometrium: a microarray analysis in clomiphene citrate-treated and artificial menstrual cycles. J Clin Endocrinol Metab 2011;96:1737-46.
15. KIM JY, SONG H, KIM H, et al. Transcriptional profiling with a pathway-oriented analysis identifies dysregulated molecular phenotypes in the endometrium of patients with polycystic ovary syndrome. J Clin Endocrinol Metab 2009;94:1416-26.
16. PATEL B, ELGUERO S, THAKORE S, DAHOUD W, BEDAIWY M, MESIANO S. Role of nuclear progesterone receptor isoforms in uterine pathophysiology. Hum Reprod Update 2015;21:155-73.
17. GELLERSEN B, BROSENS JJ. Cyclic decidualization of the human endometrium in reproductive health and failure. Endocr Rev 2014;35:851-905.
18. MARGARIT L, TAYLOR A, ROBERTS MH, et al. MUC1 as a discriminator between endometrium from fertile and infertile patients with PCOS and endometriosis. J Clin Endocrinol Metab 2010;95:5320-9.
19. QUEZADA S, AVELLAIRA C, JOHNSON MC, et al. Evaluation of steroid receptors, coregulators, and molecules associated with uterine receptivity in secretory

endometria from untreated women with polycystic ovary syndrome. Fertil Steril 2006;85:1017-26.

20. THIENEL T, CHWALISZ K, WINTERHAGER E. Expression of MAPkinases (Erk1/2) during decidualization in the rat: regulation by progesterone and nitric oxide. Mol Hum Reprod 2002;8:465-74.
21. LEE CH, KIM TH, LEE JH, et al. Extracellular signal-regulated kinase 1/2 signaling pathway is required for endometrial decidualization in mice and human. PLoS One 2013;8:e75282.
22. TAPIA-PIZARRO A, ARCHILES S, ARGANDONA F, et al. hCG activates Epac-Erk1/2 signaling regulating Progesterone Receptor expression and function in human endometrial stromal cells. Mol Hum Reprod 2017;23:393-405.
23. NADERPOOR N, SHORAKAE S, DE COURTEN B, MISSO ML, MORAN LJ, TEEDE HJ. Metformin and lifestyle modification in polycystic ovary syndrome: systematic review and meta-analysis. Hum Reprod Update 2015;21:560-74.
24. JAKUBOWICZ DJ, SEPPALA M, JAKUBOWICZ S, et al. Insulin reduction with metformin increases luteal phase serum glycodelin and insulin-like growth factor-binding protein 1 concentrations and enhances uterine vascularity and blood flow in the polycystic ovary syndrome. J Clin Endocrinol Metab 2001;86:1126-33.
25. LI X, GUO JR, LIN JF, FENG Y, BILLIG H, SHAO R. Combination of Diane-35 and metformin to treat early endometrial carcinoma in PCOS women with insulin resistance. J Cancer 2014;5:173-81.
26. PALOMBA S, RUSSO T, ORIO F, JR., et al. Uterine effects of metformin administration in anovulatory women with polycystic ovary syndrome. Hum Reprod 2006;21:457-65.
27. MCNEILLY AS, DUNCAN WC. Rodent models of polycystic ovary syndrome. Mol Cell Endocrinol 2013;373:2-7.
28. ZHANG Y, HU M, MENG F, et al. Metformin Ameliorates Uterine Defects in a Rat Model of Polycystic Ovary Syndrome. EBioMedicine 2017;18:157-70.
29. ZHANG Y, SUN X, SUN X, et al. Molecular characterization of insulin resistance and glycolytic metabolism in the rat uterus. Sci Rep 2016;6:30679.
30. LI X, CUI P, JIANG HY, et al. Reversing the reduced level of endometrial GLUT4 expression in polycystic ovary syndrome: a mechanistic study of metformin action. Am J Transl Res 2015;7:574-86.
31. Rotterdam ESHRE/ASRM-Sponsored PCOS consensus workshop group. Revised 2003 consensus on diagnostic criteria and long-term health risks related to polycystic ovary syndrome (PCOS). Hum Reprod 2004;19:41-7.
32. LI X, PISHDARI B, CUI P, et al. Regulation of Androgen Receptor Expression Alters AMPK Phosphorylation in the Endometrium: In Vivo and In Vitro Studies in Women with Polycystic Ovary Syndrome. Int J Bio Sci 2015;11:1376-89.
33. NOYES RW, HERTIG AT, ROCK J. Dating the endometrial biopsy. Am J Obstet Gynecol 1975;122:262-3.
34. FENG Y, WEIJDEGARD B, WANG T, et al. Spatiotemporal expression of androgen receptors in the female rat brain during the oestrous cycle and the impact of exogenous androgen administration: a comparison with gonadally intact males. Mol Cell Endocrinol 2010;321:161-74.
35. DAMARIO MA, BOGOVICH K, LIU HC, ROSENWAKS Z, PORETSKY L. Synergistic effects of insulin-like growth factor-I and human chorionic gonadotropin in the rat ovary. Metabolism 2000;49:314-20.
36. PORETSKY L, CLEMONS J, BOGOVICH K. Hyperinsulinemia and human chorionic gonadotropin synergistically promote the growth of ovarian follicular cysts in rats. Metabolism 1992;41:903-10.

37. BOGOVICH K, CLEMONS J, PORETSKY L. Insulin has a biphasic effect on the ability of human chorionic gonadotropin to induce ovarian cysts in the rat. Metabolism 1999;48:995-1002.
38. KIM HJ, LEE GS, JI YK, CHOI KC, JEUNG EB. Differential expression of uterine calcium transporter 1 and plasma membrane Ca2+ ATPase 1b during rat estrous cycle. Am J Physiol Endocrinol Metab 2006;291:E234-41.
39. KNOX KL, RINGSTROM SJ, SZABO M, et al. RU486 on an estrogen background blocks the rise in serum follicle-stimulating hormone induced by antiserum to inhibin or ovariectomy. Endocrinology 1996;137:1226-32.
40. CUI P, LI X, WANG X, et al. Lack of cyclical fluctuations of endometrial GLUT4 expression in women with polycystic ovary syndrome: Evidence for direct regulation of GLUT4 by steroid hormones. BBA clinical 2015;4:85-91.
41. MARIEE N, LI TC, LAIRD SM. Expression of leukaemia inhibitory factor and interleukin 15 in endometrium of women with recurrent implantation failure after IVF; correlation with the number of endometrial natural killer cells. Hum Reprod 2012;27:1946-54.
42. AVELLAIRA C, VILLAVICENCIO A, BACALLAO K, et al. Expression of molecules associated with tissue homeostasis in secretory endometria from untreated women with polycystic ovary syndrome. Hum Reprod 2006;21:3116-21.
43. BHURKE AS, BAGCHI IC, BAGCHI MK. Progesterone-Regulated Endometrial Factors Controlling Implantation. Am J Reprod Immunol 2016;75:237-45.
44. WIRA CR, FAHEY JV, SENTMAN CL, PIOLI PA, SHEN L. Innate and adaptive immunity in female genital tract: cellular responses and interactions. Immunol Rev 2005;206:306-35.
45. BRENNER RM, SLAYDEN OD, RODGERS WH, et al. Immunocytochemical assessment of mitotic activity with an antibody to phosphorylated histone H3 in the macaque and human endometrium. Hum Reprod 2003;18:1185-93.
46. TRANGUCH S, WANG H, DAIKOKU T, XIE H, SMITH DF, DEY SK. FKBP52 deficiency-conferred uterine progesterone resistance is genetic background and pregnancy stage specific. J Clin Invest 2007;117:1824-34.
47. YANG Z, WOLF IM, CHEN H, et al. FK506-binding protein 52 is essential to uterine reproductive physiology controlled by the progesterone receptor A isoform. Mol Endocrinol 2006;20:2682-94.
48. MUKHERJEE A, AMATO P, ALLRED DC, DEMAYO FJ, LYDON JP. Steroid receptor coactivator 2 is required for female fertility and mammary morphogenesis: insights from the mouse, relevance to the human. Nucl Rec Signal 2007;5:e011.
49. MUKHERJEE A, SOYAL SM, FERNANDEZ-VALDIVIA R, et al. Steroid receptor coactivator 2 is critical for progesterone-dependent uterine function and mammary morphogenesis in the mouse. Mol Cell Biol 2006;26:6571-83.
50. ESCOBAR-MORREALE HF, LUQUE-RAMIREZ M, GONZALEZ F. Circulating inflammatory markers in polycystic ovary syndrome: a systematic review and metaanalysis. Fertil Steril 2011;95:1048-58 e1-2.
51. LIU M, GAO J, ZHANG Y, et al. Serum levels of TSP-1, NF-kappaB and TGF-beta1 in polycystic ovarian syndrome (PCOS) patients in northern China suggest PCOS is associated with chronic inflammation. Clin Endocrinol (Oxf) 2015;83:913-22.
52. PILTONEN TT, CHEN J, ERIKSON DW, et al. Mesenchymal stem/progenitors and other endometrial cell types from women with polycystic ovary syndrome (PCOS) display inflammatory and oncogenic potential. J Clin Endocrinol Metab 2013;98:3765-75.

53. OROSTICA L, ASTORGA I, PLAZA-PARROCHIA F, et al. Proinflammatory environment and role of TNF-alpha in endometrial function of obese women having polycystic ovarian syndrome. Int J Obes 2016;40:1715-22.
54. PILTONEN TT, CHEN JC, KHATUN M, et al. Endometrial stromal fibroblasts from women with polycystic ovary syndrome have impaired progesterone-mediated decidualization, aberrant cytokine profiles and promote enhanced immune cell migration in vitro. Hum Reprod 2015;30:1203-15.
55. GRANDI G, MUELLER M, BERSINGER N, et al. Progestin suppressed inflammation and cell viability of tumor necrosis factor-alpha-stimulated endometriotic stromal cells. Am J Reprod Immunol 2016;76:292-8.
56. SHOELSON SE, LEE J, GOLDFINE AB. Inflammation and insulin resistance. J Clin Invest 2006;116:1793-801.
57. SPRITZER PM, LECKE SB, SATLER F, MORSCH DM. Adipose tissue dysfunction, adipokines, and low-grade chronic inflammation in polycystic ovary syndrome. Reproduction 2015;149:R219-27.
58. LAN CW, CHEN MJ, TAI KY, et al. Functional microarray analysis of differentially expressed genes in granulosa cells from women with polycystic ovary syndrome related to MAPK/ERK signaling. Sci Rep 2015;5:14994.
59. NELSON-DEGRAVE VL, WICKENHEISSER JK, HENDRICKS KL, et al. Alterations in mitogen-activated protein kinase kinase and extracellular regulated kinase signaling in theca cells contribute to excessive androgen production in polycystic ovary syndrome. Mol Endocrinol 2005;19:379-90.
60. ARTHUR JS, LEY SC. Mitogen-activated protein kinases in innate immunity. Nat Rev Immunol 2013;13:679-92.
61. CUADRADO A, NEBREDA AR. Mechanisms and functions of p38 MAPK signalling. Biochem J 2010;429:403-17.
62. MATTEO M, SERVIDDIO G, MASSENZIO F, et al. Reduced percentage of natural killer cells associated with impaired cytokine network in the secretory endometrium of infertile women with polycystic ovary syndrome. Fertil Steril 2010;94:2222-7, 27 e1-3.
63. ZHAO Y, ZHANG C, HUANG Y, et al. Up-regulated expression of WNT5a increases inflammation and oxidative stress via PI3K/AKT/NF-kappaB signaling in the granulosa cells of PCOS patients. J Clin Endocrinol Metab 2015;100:201-11.

Figure legends

Figure 1. Comparison of the expression and localization of endometrial PGR isoforms, ERα, and cellular marker proteins in women with and without PCOS. A, Quantitative RT-PCR analysis of *PGR* and *PGRB* mRNA levels in the proliferative phase between non-PCOS (n = 9) and PCOS (n = 6) patients. mRNA levels were normalized to the average level of *ACTB* (β-actin) and *CYC1* (cytochrome c isoform 1) in the same sample. Values are expressed as means ± SEM. Statistical tests are described in the Materials and Methods. * $p < 0.05$; ** $p < 0.01$. B, Western blot analysis of protein expression in the human endometrial tissues was performed. Representative images and quantification of the densitometric data for PGRA, PGRB, ERα, cytokeratin 8 (an epithelial cell marker), vimentin (a mesenchymal/stromal cell marker), and β-actin expression are shown (n = 5/group). Values are expressed as means ± SEM. Statistical tests are described in the Materials and Methods. * $p < 0.05$; ** $p < 0.01$. C, Immunohistochemical and immunofluorescent staining of PGR, PGRB, ERα, cytokeratin 8, vimentin, and Ki-67 in the endometrial tissue sections from non-PCOS (n = 5) and PCOS (n = 3) patients. The tissue sections were counterstained with hematoxylin. Ge, glandular epithelial cells; Str, stromal cells. Scale bars (100 μm) are indicated in the photomicrographs.

Figure 2. Chronic treatment with metformin alters PGR isoform protein expression and PGR-target gene expression in the rat uterus *in vivo*. A, Western blot analysis of protein expression in the rat uterus was performed. Representative images and quantification of the densitometric data (n = 8–9/group) of PGR isoforms are shown. B, Immunohistochemical detection of PGR in control rats treated with saline or metformin and in insulin+hCG-treated rats treated with saline or metformin. Representative images (n = 5/group) are shown. Lu, lumen; Le, luminal epithelial cells; Ge, glandular epithelial cells; Str, stromal cells. Scale bars (100 μm) are indicated in the photomicrographs. High magnification images are shown in the

bottom panels. C, Uterine tissues from control rats treated with vehicle or metformin and insulin+hCG-treated rats treated with saline or metformin (n = 6/group) were analyzed for mRNA levels of *Ihh*, *Ptch*, *Smo*, *Nr2f2*, *Hand2*, *Fkbp52*, and *Ncoa2* by qRT-PCR. The mRNA level of each gene relative to the mean of the sum of the *Gapdh* and *U87* mRNA levels in the same sample is shown. Values are expressed as means ± SEM. Statistical tests are described in the Material and Methods. * $p < 0.05$; ** $p < 0.01$; *** $p < 0.001$.

Figure 3. Chronic treatment with metformin alters PGR isoform protein expression and PGR-target gene expression in the rat uterus after implantation. A, Western blot analysis of protein expression in the rat uterus was performed. Representative images and quantification of the densitometric data of PR isoforms are shown (n = 5–7/group). B, Immunohistochemical detection of PGR in the uterine implantation and inter-implantation sites. Representative images are shown (n = 5/group). DS, decidualized stroma; Lu, lumen; Le, luminal epithelial cells; Ge, glandular epithelial cells; Str, stromal cells. Scale bars (100 μm) are indicated in the photomicrographs. C, Uterine tissues (n = 5–6/group) were analyzed for mRNA levels of *Ihh*, *Ptch*, *Smo*, *Nr2f2*, *Hand2*, *Fkbp52*, and *Ncoa2* by qRT-PCR. The mRNA level of each gene is shown relative to the mean of the sum of the *Gapdh* and *U87* mRNA levels in the same sample. Values are expressed as means ± SEM. Statistical tests are described in the Materials and Methods. * $p < 0.05$; ** $p < 0.01$; *** $p < 0.001$.

Figure 4. Specific regulation of uterine PGR isoforms and PGR-targeted gene expression by metformin treatment *in vitro*. Quantitative RT-PCR analysis of *Pgr*, *Pgrb*, *Ihh*, *Ptch*, *Smo*, *Nr2f2*, *Hand2*, *Fkbp52*, and *Ncoa2* mRNA levels in rat uterine tissues treated with either saline or 10 mM metformin for the indicated culture times (n = 6/group). mRNA levels were normalized to the average levels of *Gapdh* and *U87* mRNA in the same sample. Values are expressed as means ± SEM. Statistical tests are described in the Materials and Methods. * $p < 0.05$; ** $p < 0.01$; *** $p < 0.001$.

Figure 5. Specific regulation of implantation-related gene expression by metformin treatment *in vitro*. Quantitative RT-PCR analysis of *Prl*, *Igfbp1*, *Lif*, *Il11*, *Pc6*, *Spp1*, *Maoa*, *Ednrb*, *Hoxa10*, *Hoxa11*, *Lrh1*, *Sgk1*, *Hbegf*, and *Krt13* mRNA levels in rat uterine tissues treated with either saline or 10 mM metformin for the indicated culture times (n = 6/group). mRNA levels were normalized to the average levels of *Gapdh* and *U87* mRNA in the same sample. Values are expressed as means ± SEM. Statistical tests are described in the Materials and Methods. * $p < 0.05$; ** $p < 0.01$; *** $p < 0.001$.

Figure 6. Specific regulation of uterine PGR isoforms and PGR-targeted gene expression by treatment with P4 and/or RU486 *in vivo*. Uterine tissues (n = 5–6/group) were analyzed for mRNA levels of *Pgr*, *Pgrb*, *Ihh*, *Ptch*, *Smo*, *Nr2f2*, *Hand2*, *Fkbp52*, and *Ncoa2* by qRT-PCR. mRNA levels were normalized to the average levels of *Gapdh* and *U87* mRNA in the same sample. Values are expressed as means ± SEM. Statistical tests are described in the Materials and Methods. * $p < 0.05$; ** $p < 0.01$; *** $p < 0.001$.

Figure 7. Chronic treatment with metformin alters the MAPK signaling pathway in the rat uterus before and after implantation. Western blot analysis of protein expression in the rat uterus was performed. Representative images and quantification of the densitometric data for p-c-Raf, p-MEK1/2, p-ERK1/2, ERK1/2, p-p38 MAPK, and p38 MAPK are shown (n = 6–9/group before implantation; n = 5–6/group after implantation). Values are expressed as means ± SEM. Statistical tests are described in the Materials and Methods. * $p < 0.05$; ** $p < 0.01$.

Figure 8. Chronic treatment with metformin alters ER subtype mRNA and protein expression in the rat uterus *in vivo*. A, Uterine tissues from control rats treated with saline vehicle or metformin and insulin+hCG-treated rats treated with saline or metformin (n = 6/group) were analyzed for mRNA levels of *Esr1* (ERα) and *Esr2* (ERβ) by qRT-PCR. The mRNA level of each gene relative to the mean of the sum of the *Gapdh* and *U87* mRNA

levels in the same sample is shown. Values are expressed as means ± SEM. Statistical tests are described in the Material and Methods. * $p < 0.05$; ** $p < 0.01$; *** $p < 0.001$. B, Immunofluorescence detection of ERα (red) and ERβ (green) in control rats treated with saline (B1-2) or metformin (C1-2) and in insulin+hCG-treated rats treated with saline (D1-2) or metformin (E1-2). Representative images are shown (n = 5/group). Cell nuclei were counterstained with DAPI (blue, lower panel). Lu, lumen; Le, luminal epithelial cells; Ge, glandular epithelial cells; Str, stromal cells. Scale bars (100 μm) are indicated in the photomicrographs.

Figure 9. Chronic treatment with metformin alters ER subtype mRNA and protein expression in the rat uterus after implantation. A, Uterine tissues from control rats treated with saline or metformin and insulin+hCG-treated rats treated with saline or metformin (n = 5/group) were analyzed for mRNA levels of *Esr1* (ERα) and *Esr2* (ERβ) by qRT-PCR. The mRNA level of each gene relative to the mean of the sum of the *Gapdh* and *U87* mRNA levels in the same sample is shown. Values are expressed as means ± SEM. Statistical tests are described in the Materials and Methods. * $p < 0.05$; ** $p < 0.01$. B, Immunofluorescence detection of ERα (red) and ERβ (green) in control rats treated with saline (B1-2) or metformin (C1-2) and in insulin+hCG-treated rats treated with metformin with implantation (D1-2) or without implantation (E1). Representative images are shown (n = 5/group). Cell nuclei were counterstained with DAPI (blue, lower panel). DS, decidualized stroma; Lu, lumen; Le, luminal epithelial cells; Ge, glandular epithelial cells; Str, stromal cells. Scale bars (100 μm) are indicated in the photomicrographs.

Figure 1

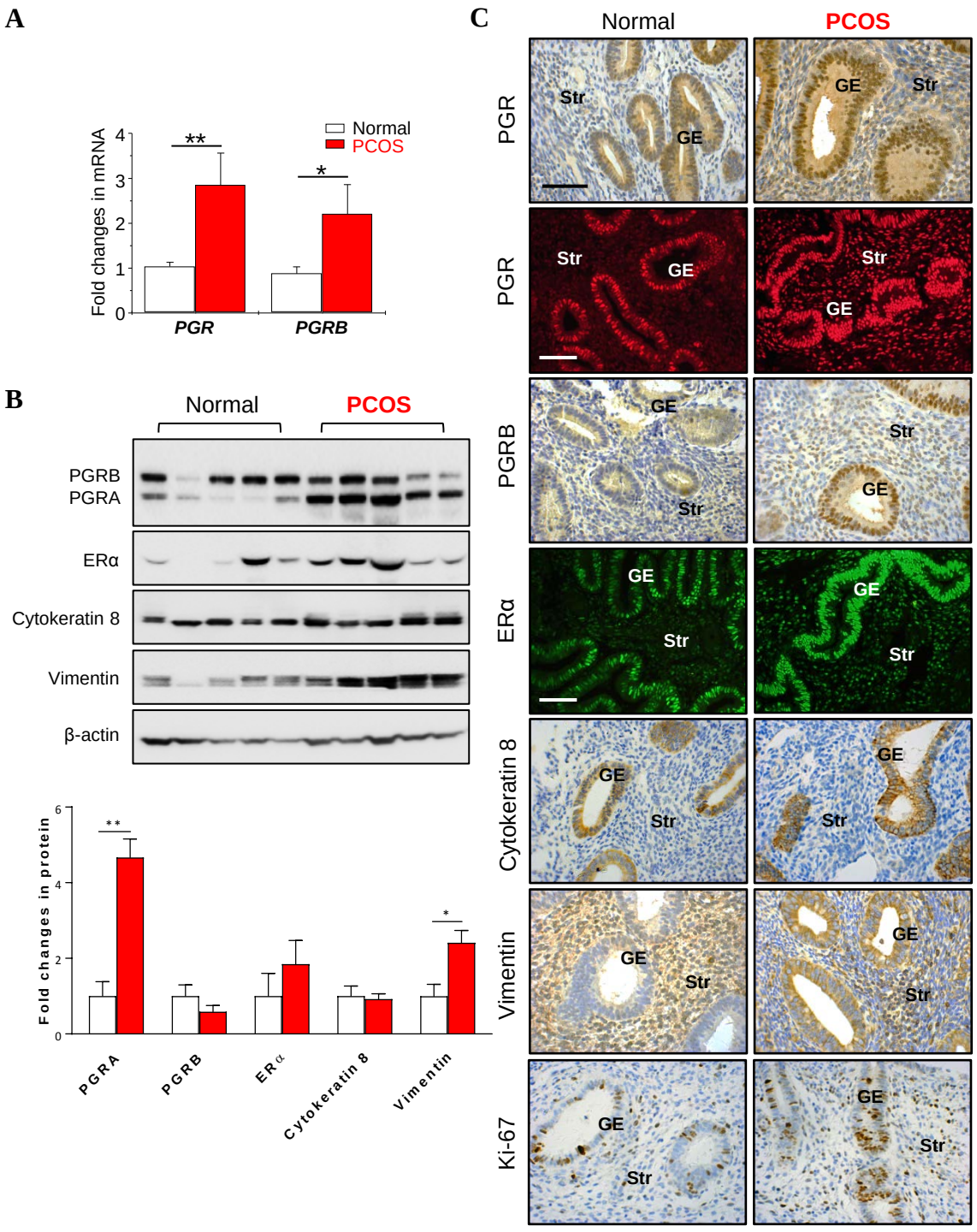
A
Fold changes in mRNA
Normal
PCOS
**
*
PGR
PGRB
B
Normal
PCOS
PGRB
PGRA
ERα
Cytokeratin 8
Vimentin
β-actin
Fold changes in protein
**
*
PGRA
PGRB
ERα
Cytokeratin 8
Vimentin
C
Normal
PCOS
PGR
PGR
PGRB
ERα
Cytokeratin 8
Vimentin
Ki-67
Str
GE

Figure 2

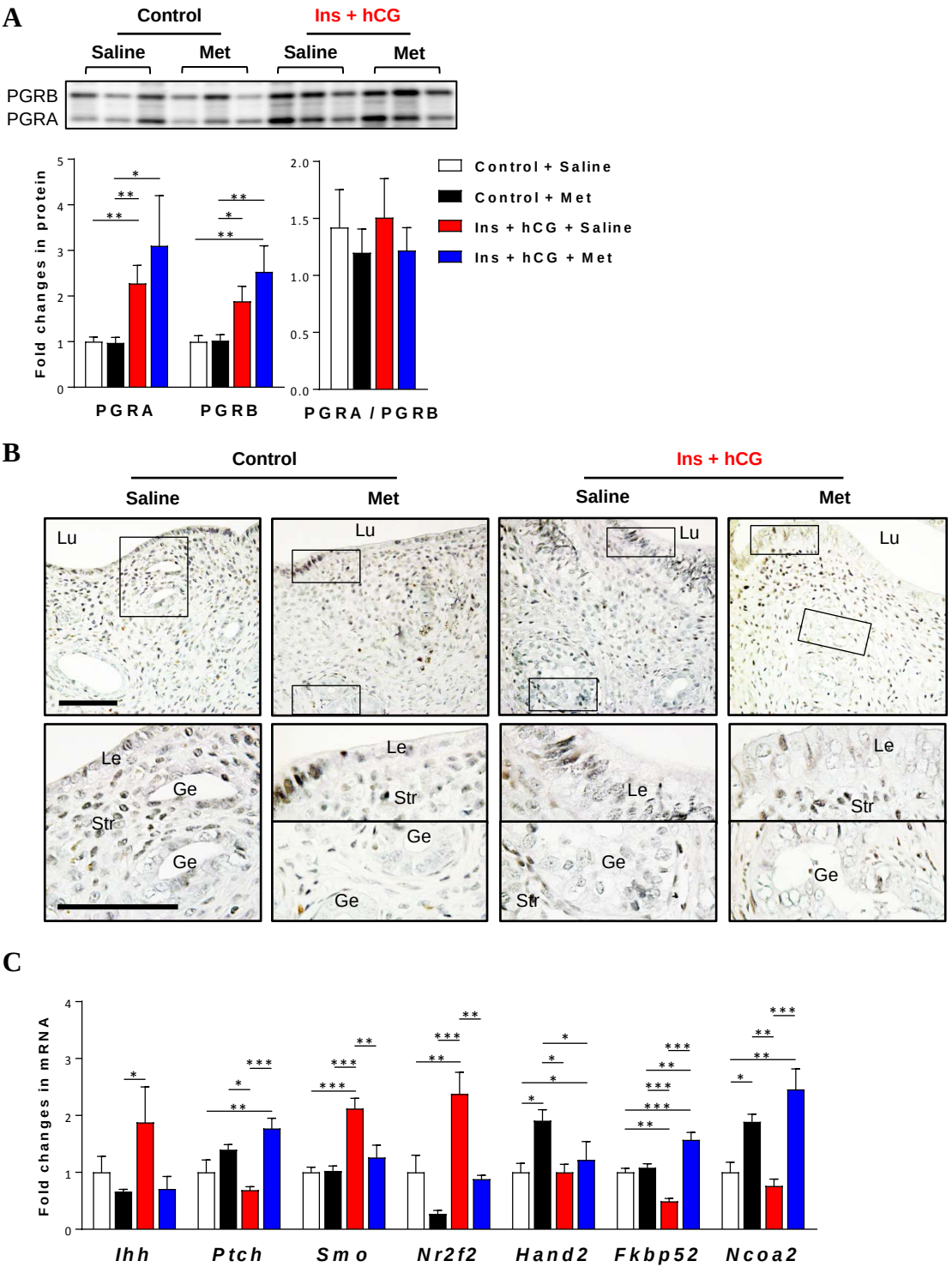
A
Control
Ins + hCG
Saline
Met
Saline
Met
PGRB
PGRA
Fold changes in protein
PGRA
PGRB
PGRA / PGRB
Control + Saline
Control + Met
Ins + hCG + Saline
Ins + hCG + Met
B
Control
Ins + hCG
Saline
Met
Saline
Met
Lu
Le
Ge
Str
C
Fold changes in mRNA
Ihh
Ptch
Smo
Nr2f2
Hand2
Fkbp52
Ncoa2

Figure 3

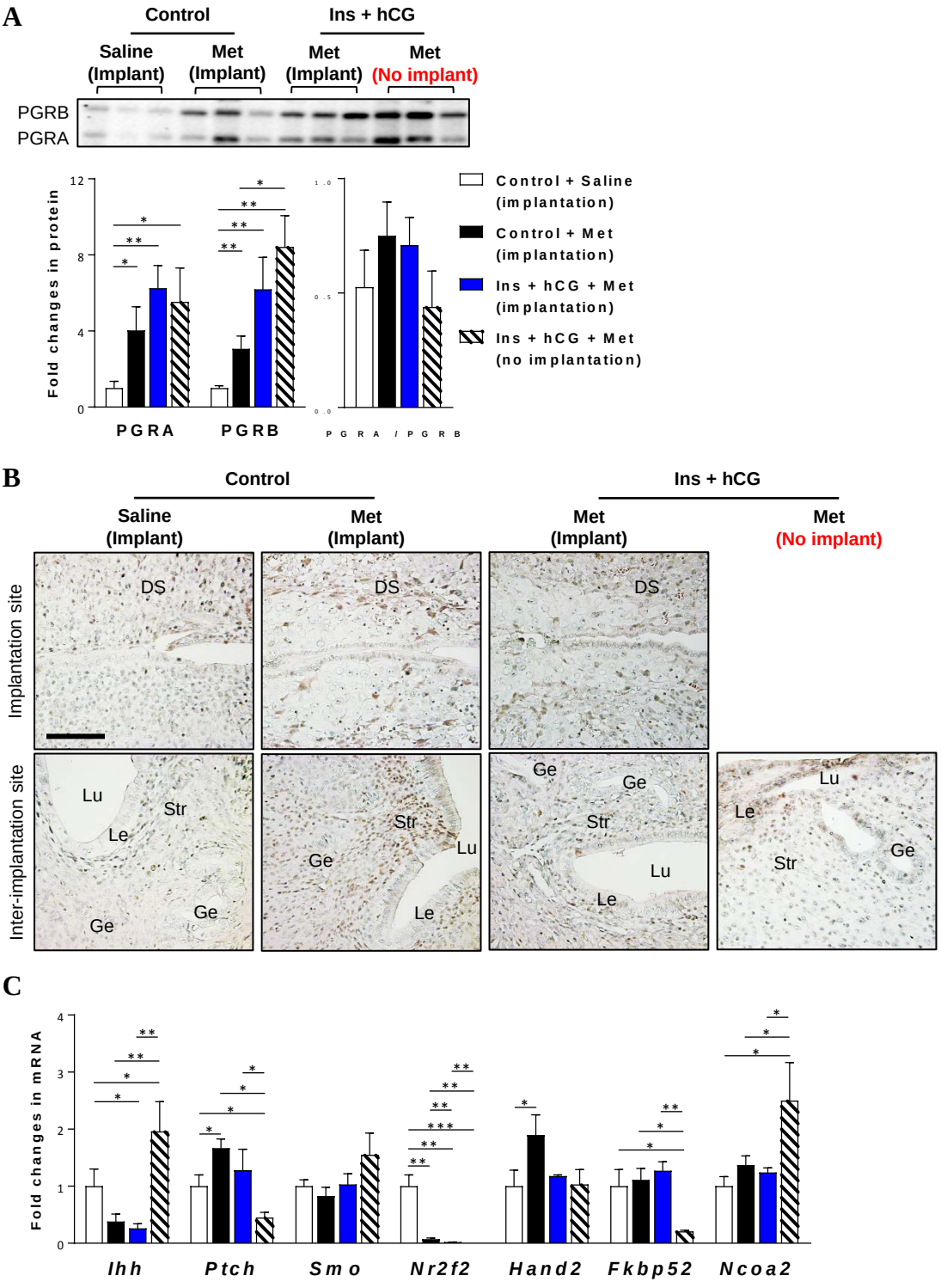
A
Control
Ins + hCG
Saline (Implant)
Met (Implant)
Met (Implant)
Met (No implant)
PGRB
PGRA
Fold changes in protein
PGRA
PGRB
PGRA / PGRB
Control + Saline (implantation)
Control + Met (implantation)
Ins + hCG + Met (implantation)
Ins + hCG + Met (no implantation)
B
Control
Ins + hCG
Saline (Implant)
Met (Implant)
Met (Implant)
Met (No implant)
Implantation site
Inter-implantation site
DS
Lu
Str
Le
Ge
C
Fold changes in mRNA
Ihh
Ptch
Smo
Nr2f2
Hand2
Fkbp52
Ncoa2

Figure 4

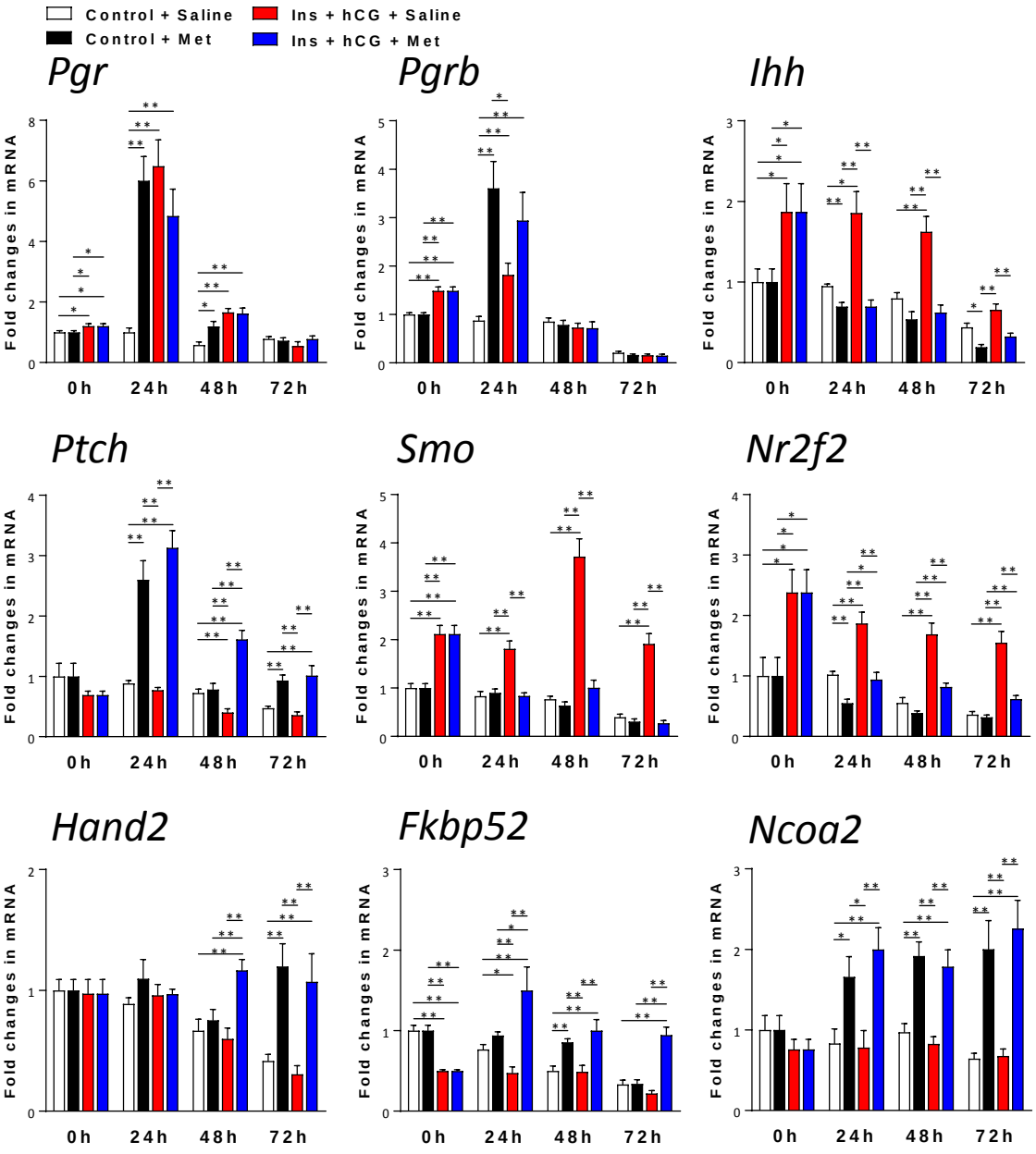
Control + Saline
Control + Met
Ins + hCG + Saline
Ins + hCG + Met
Pgr
Pgrb
Ihh
Ptch
Smo
Nr2f2
Hand2
Fkbp52
Ncoa2
Fold changes in mRNA
0h
24h
48h
72h

Figure 5

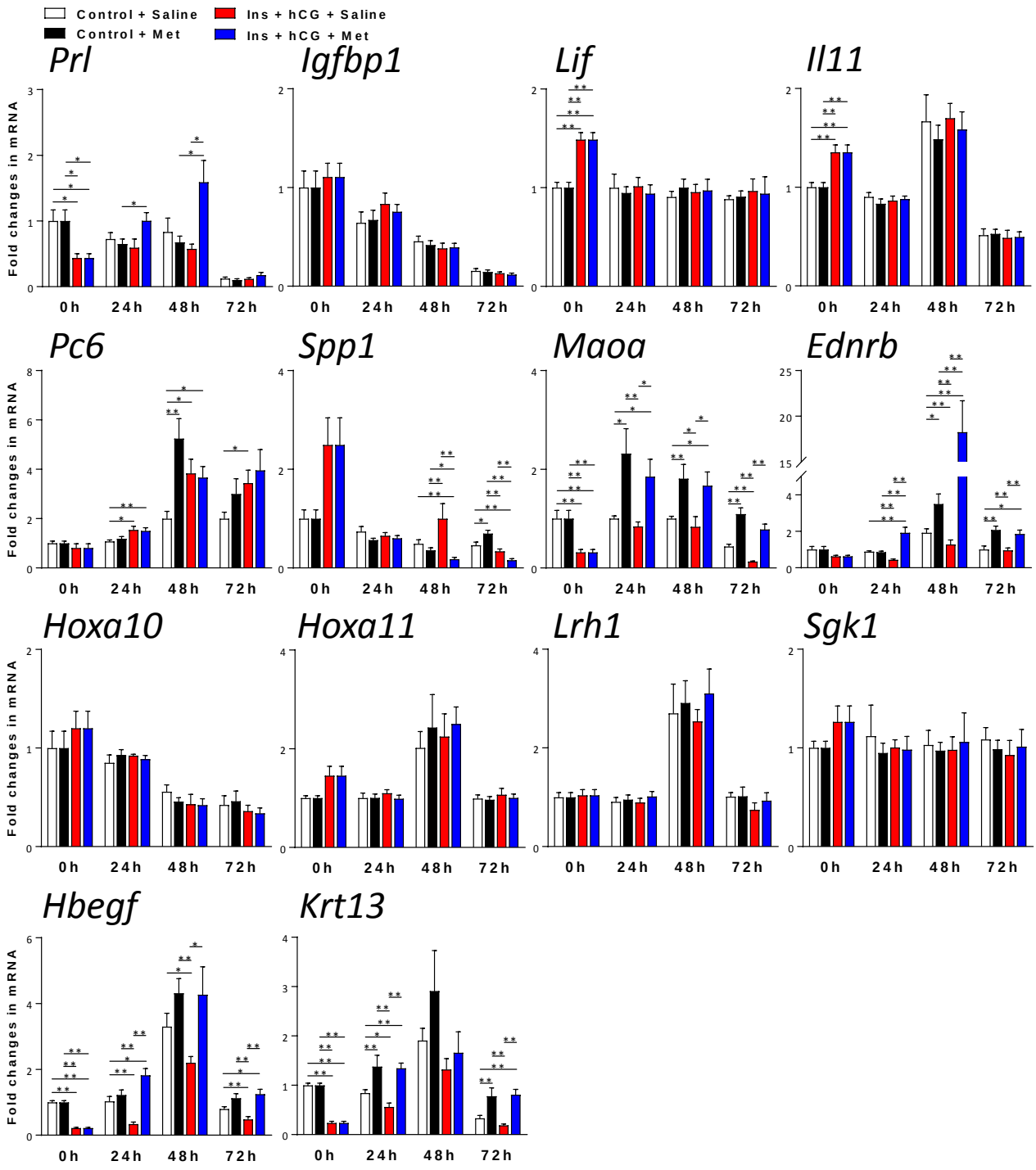
Control + Saline
Control + Met
Ins + hCG + Saline
Ins + hCG + Met
Prl
Igfbp1
Lif
Il11
Pc6
Spp1
Maoa
Ednrb
Hoxa10
Hoxa11
Lrh1
Sgk1
Hbegf
Krt13
Fold changes in mRNA
0h
24h
48h
72h

Figure 6

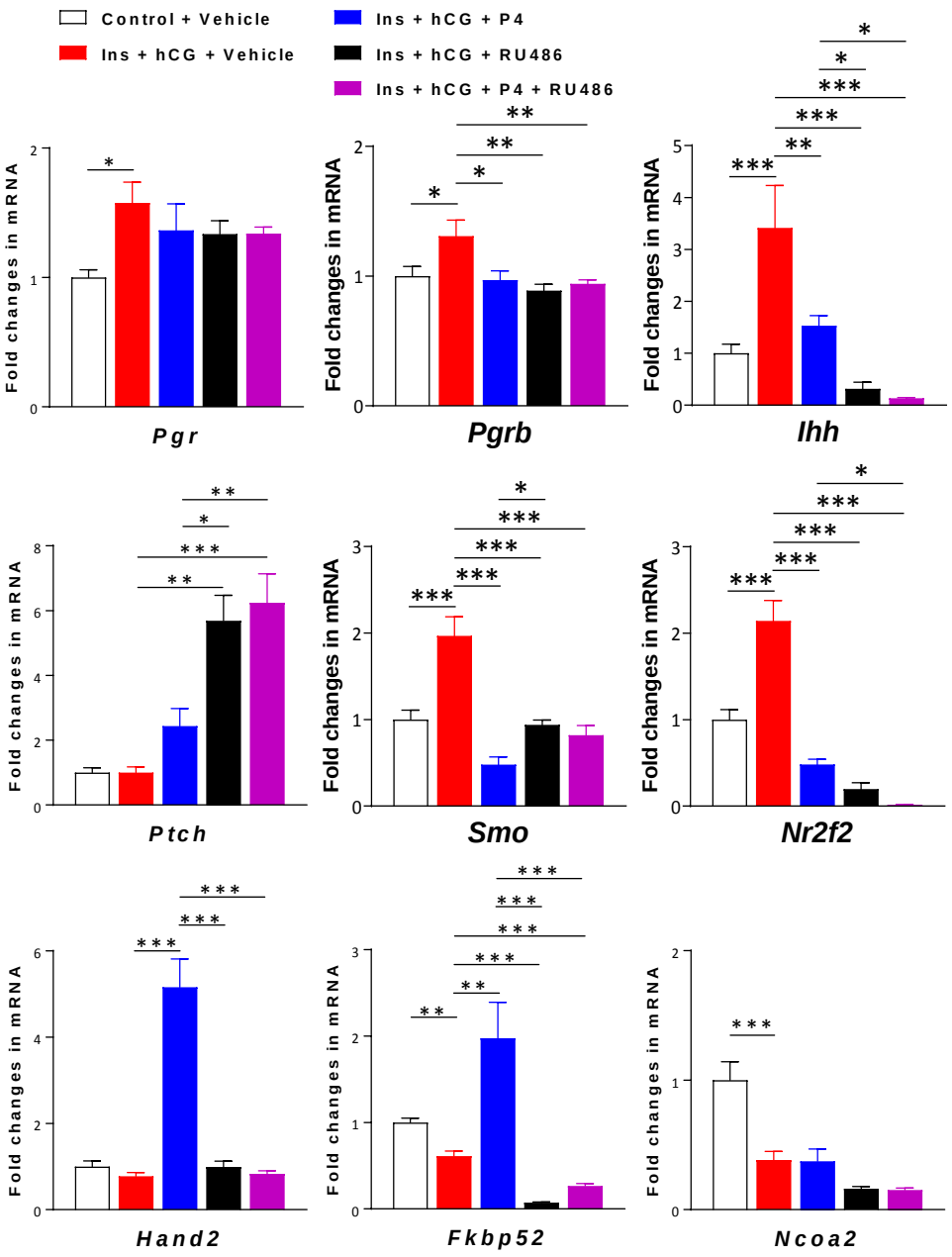
Control + Vehicle
Ins + hCG + Vehicle
Ins + hCG + P4
Ins + hCG + RU486
Ins + hCG + P4 + RU486
Fold changes in mRNA
Pgr
Pgrb
Ihh
Ptch
Smo
Nr2f2
Hand2
Fkbp52
Ncoa2

Figure 7

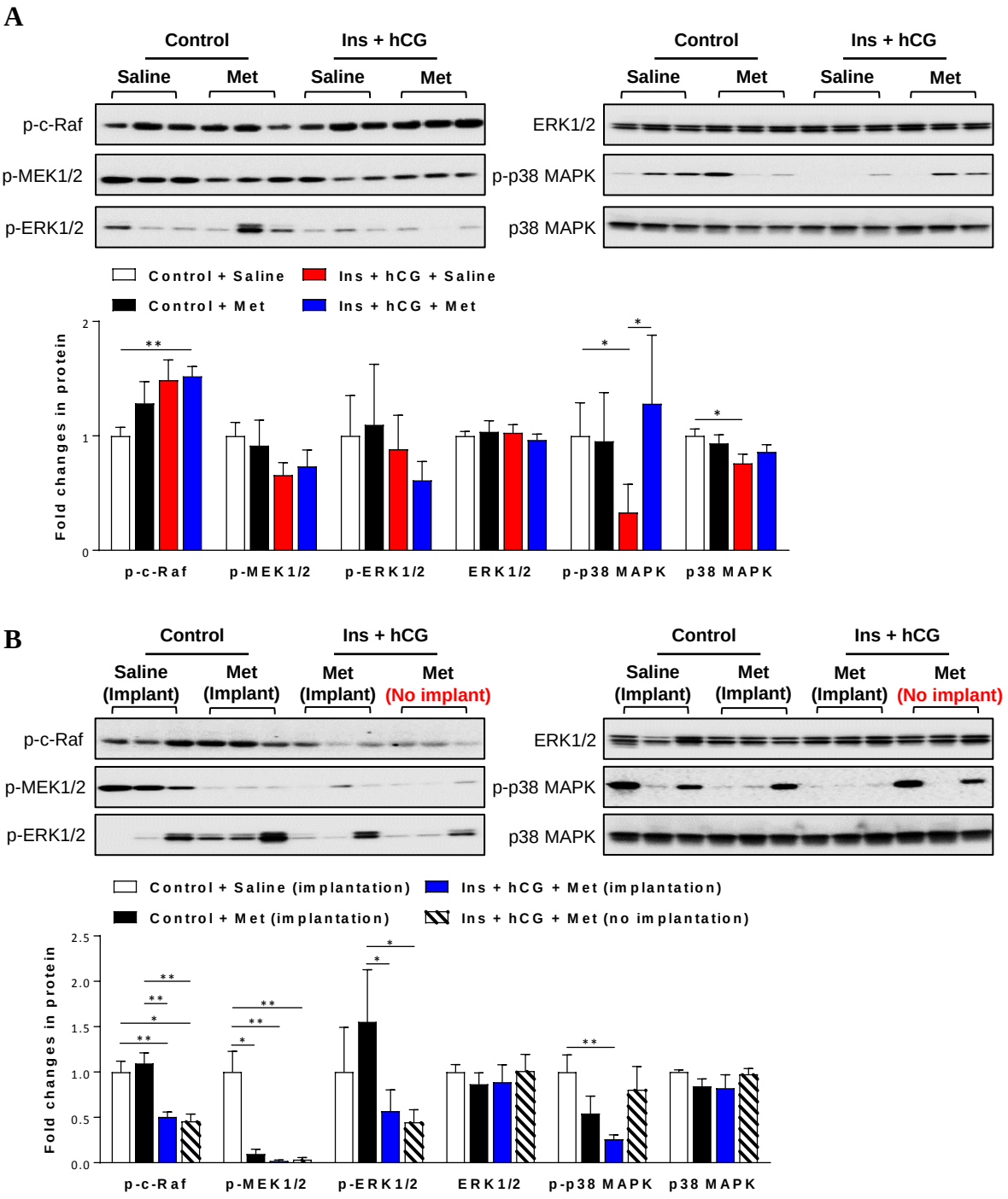
A
Control
Ins + hCG
Saline
Met
Saline
Met
p-c-Raf
p-MEK1/2
p-ERK1/2
ERK1/2
p-p38 MAPK
p38 MAPK
Control + Saline
Ins + hCG + Saline
Control + Met
Ins + hCG + Met
Fold changes in protein
p-c-Raf
p-MEK1/2
p-ERK1/2
ERK1/2
p-p38 MAPK
p38 MAPK
B
Control
Ins + hCG
Saline (Implant)
Met (Implant)
Met (Implant)
Met (No implant)
Control + Saline (implantation)
Ins + hCG + Met (implantation)
Control + Met (implantation)
Ins + hCG + Met (no implantation)
Fold changes in protein

Figure 8

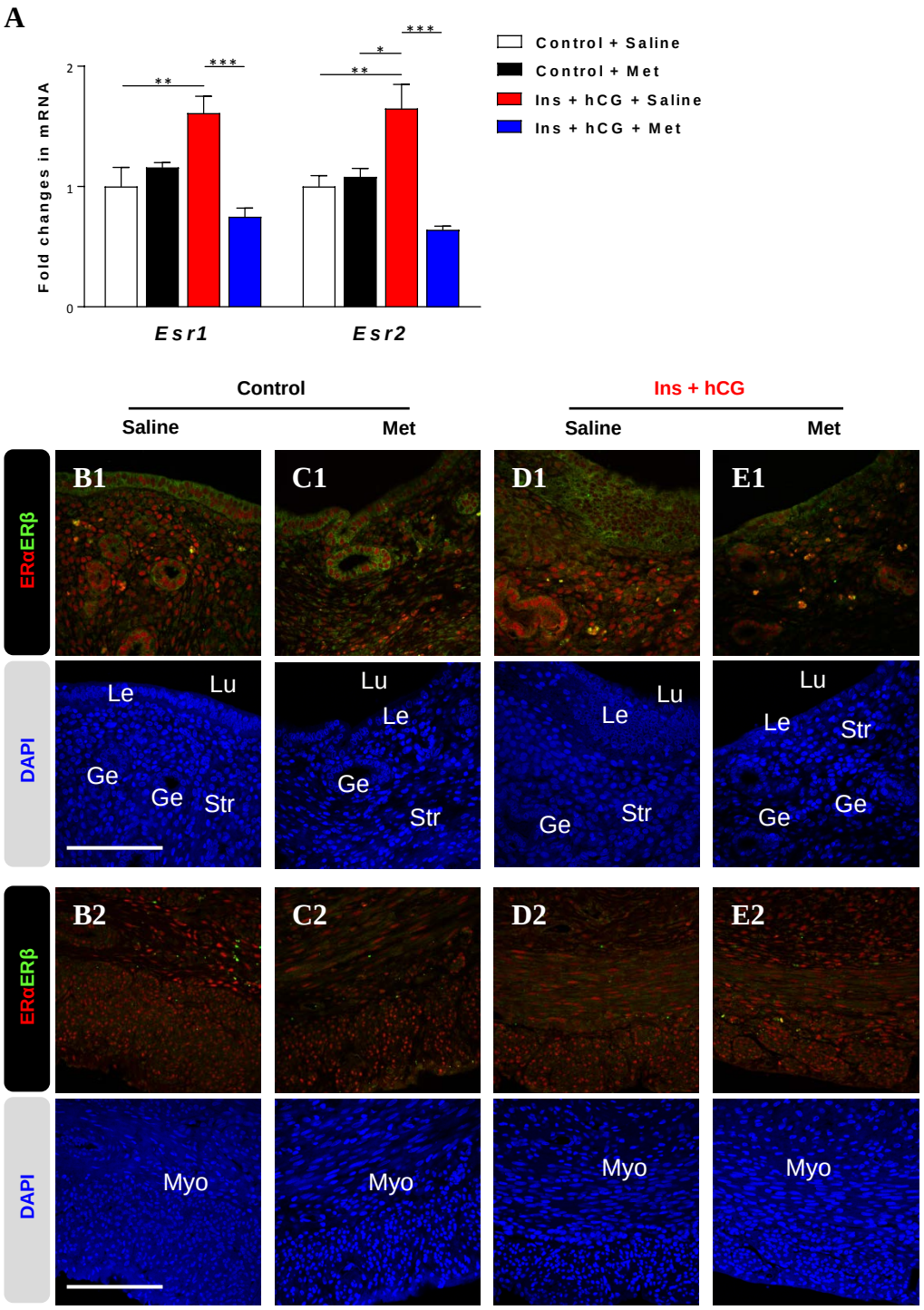
A
Fold changes in mRNA
2
1
0
**
***
**
*
***
Esr1
Esr2
Control + Saline
Control + Met
Ins + hCG + Saline
Ins + hCG + Met
Control
Ins + hCG
Saline
Met
Saline
Met
ERαERβ
DAPI
B1
C1
D1
E1
Le
Lu
Ge
Ge
Str
Lu
Le
Ge
Str
Lu
Le
Ge
Str
Lu
Le
Str
Ge
Ge
B2
C2
D2
E2
Myo
Myo
Myo
Myo

Figure 9

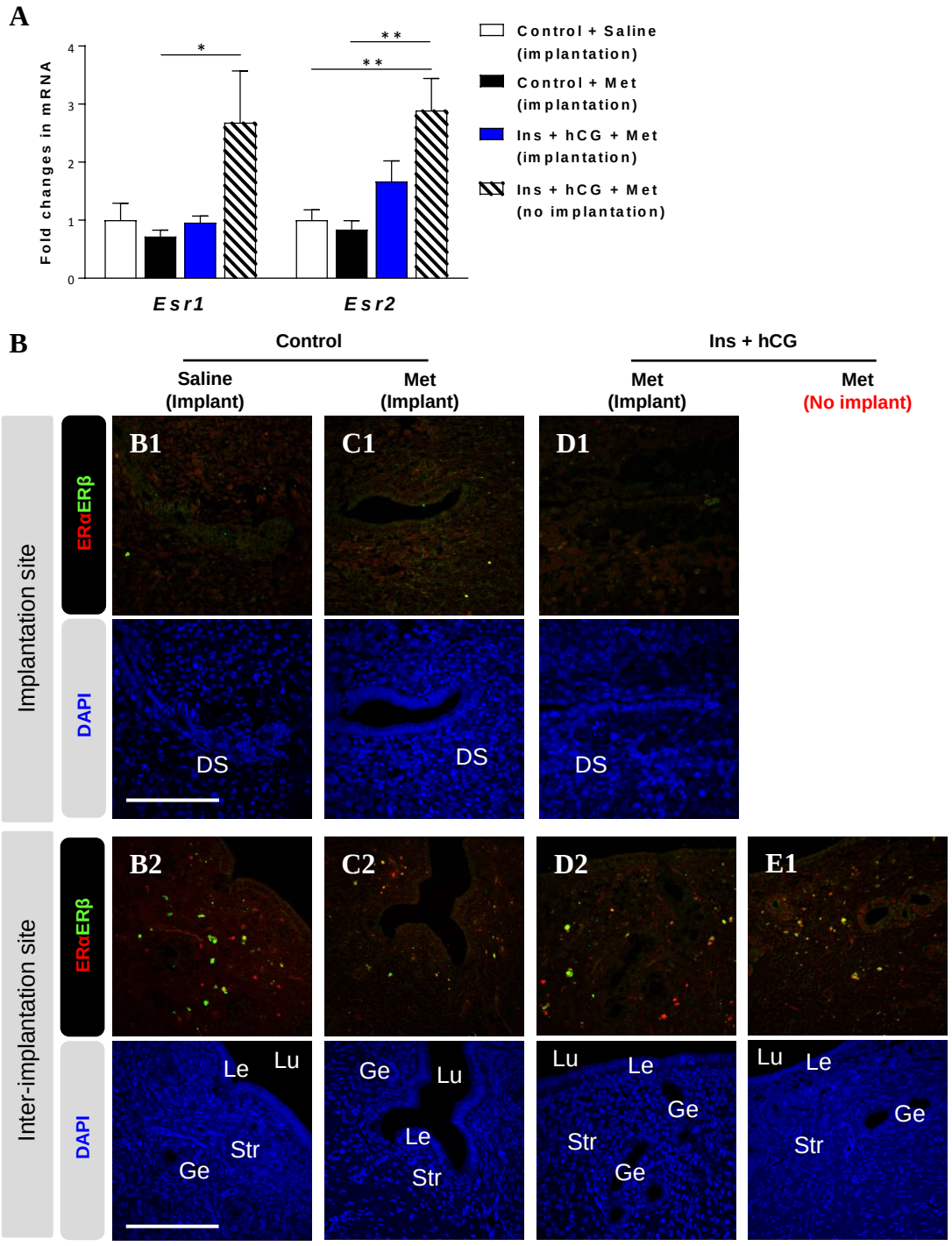
A
Fold changes in mRNA
0
1
2
3
4
*
**
**
Esr1
Esr2
Control + Saline (implantation)
Control + Met (implantation)
Ins + hCG + Met (implantation)
Ins + hCG + Met (no implantation)
B
Control
Ins + hCG
Saline (Implant)
Met (Implant)
Met (Implant)
Met (No implant)
Implantation site
Inter-implantation site
ERαERβ
DAPI
B1
C1
D1
B2
C2
D2
E1
DS
Le
Lu
Str
Ge